FC

10

REPORT NO. 740
July 1959

EFFECT OF APPENDAGE AND HULL FORM ON HYDRODYNAMIC COEFFICIENTS OF SURFACE SHIPS

by

STAVROS TSAKONAS

Davidson Laboratory
Stevens Institute of Technology
Hoboken, New Jersey

DAVIDSON LABORATORY
STEVENS INSTITUTE OF TECHNOLOGY
HOBOKEN, NEW JERSEY

EFFECT OF APPENDAGE AND HULL FORM ON HYDRODYNAMIC COEFFICIENTS OF SURFACE SHIPS

by

Stavros Tsakonas

PREPARED UNDER SPONSORSHIP OF
BUREAU OF SHIPS
FUNDAMENTAL HYDROMECHANICS RESEARCH PROGRAM
CONTRACT Nonr 263(18)
TECHNICALLY ADMINISTERED BY
DAVID TAYLOR MODEL BASIN

(DL PROJECT JU 2526)

Report No. 740

July 1959

Approved by
Paul Kaplan
Paul Kaplan
HEAD, FLUID DYNAMICS DIVISION

SUMMARY

Tests were made to determine the hydrodynamic coefficients in the yaw plane of ETT* Model 842 (of the Taylor Standard Series) with skegs of varying size, shape and position. Similar experiments were conducted with flat plates having the same profile area and geometry as the various configurations. The static and damping hydrodynamic coefficients were determined for various angles of attack by means of straight-course experiments and by interpolation of rotating-arm data. Comparison of the straight-course results with those derived by linear interpolation of the rotating-arm data show excellent agreement. This successful comparison confirms previous experience at the Davidson Laboratory that the rotating-arm can be relied upon to give hydrodynamic derivatives applicable to straight trajectories (infinite radius of turn). Consequently, straight-course motion can be considered as an intermediate between a large turn to the right and an equally large turn to the left.

Investigation of various flat plates reveals a similarity between the hydrodynamic characteristics of a model and those of a corresponding plate. These experiments show the same general trends in lateral force and yawing moment, with the exception that lateral force is larger on the plates. Reasons for this behavior are given. Comparison of experimental results with existing low aspect ratio theories substantiates the analogy believed to exist between ship hulls and wings.

An attempt to study the usefulness of the flat-plate coefficients in regard to determining the stability indices for a ship model of the same profile area is included. Comparisons of the stability indices calculated for the ship model (with its various skeg arrangements) with those obtained using the flat-plate hydrodynamic coefficients (in lieu of the model coefficients) show that this substitution cannot be made. It is concluded that the disagreement in lateral force rates between the model and plate of the same profile area is primarily responsible for the lack of agreement of the computed stability indices. This indicates that immediate practical use of the existing similarity cannot be made before a correction is applied to the magnitude of the lateral force.

Since the length and draft of a ship are taken into account in low aspect ratio analogy, while the fullness or beam is completely ignored, an immediate problem of correlating the fullness with the lateral force expression available from the low aspect ratio theories arises. The attempt to bring the results of experiments into agreement with the linear part of the low aspect theories shows that a correction factor, k , linearly dependent on the effective aspect ratio, $\mathcal{R}_e$, can be employed. It may also be seen that the factor k strongly depends on fullness of the hull, but no conclusions could be drawn on its effect, since only two different beam-length-ratio configurations were considered.

---

*Model designations applied prior to change from Experimental Towing Tank to Davidson Laboratory will be retained.

TABLE OF CONTENTS

	Page
Introduction	1
Nomenclature	4
Description of Model and Test Equipment	6
Test Program and Procedure	8
Presentation and Discussion of Data	9
Concluding Remarks and Recommendations	18
Acknowledgements	20
References	21
Tables	22
Figures	31
Appendix (Figures A-1, A-2, A-3)	62

INTRODUCTION

The problem of turning and steering of surface ships is of vital importance in the field of naval architecture since it is intimately related to maneuverability and stability and is, moreover, a special case of the general problem of the motion of bodies in fluids.

The problem of turning and course-keeping characteristics was investigated by Davidson and Schiff[1] who introduced criteria for dynamic stability based on the following assumptions:

1. the ideal incompressible fluid surrounding a ship is substantially still,
2. the linearized theory is used (cross-coupling of various effects are not considered),
3. fore and aft asymmetry together with wave-making effects are omitted.

Evaluation of these criteria is based on a priori knowledge of certain hydrodynamic coefficients which can be determined experimentally for various vessels with different appendages and various types of propulsive devices.

It has been established that the study of turning and steering of a surface ship can be restricted to the horizontal plane alone and that, for length-Froude numbers less than 0.20, wave-making effects can be neglected. Therefore, the hydrodynamic lateral force and moment coefficients are the essential parameters in turning and steering, and these can be obtained from rotating-arm tests at any speed where $F \leq 0.20$, but large enough so that Reynolds number effects are mitigated.

The requirement of optimizing the maneuverability and stability characteristics of a surface vessel makes the question of interference effects between the hull and various appendages one of fundamental importance. Theoretical work on interference of flows at wing-body and tail-body junctures has been done by aerodynamicists and to a much more limited extent by researchers[2,3] in naval architecture who have approached the analogous problem in regard to rudders in a propeller race.

This report presents the results of a model study of the hydrodynamic characteristics of ETT Model 842 of the Taylor Standard Series. Five configurations were investigated, viz., a bare hull and a hull with four different skegs. Measurements of longitudinal and lateral forces as well as

yawing moments were obtained for various angles of attack at a given speed-length ratio of 0.8.

These measurements were taken on a straight course and on a constrained circular path having a 32-foot radius. The coefficients of static and damping force derivatives along with static and damping moment derivatives were computed.

Lately, an attempt has been made to determine on theoretical grounds the forces and moments acting upon a ship by making use of the low aspect ratio wing theory. (See Fedyaevsky and Sobolev[4] and Inoue[5]) The ship hull is identified with a wing having the load waterline as its chord and twice the draft as its span. The presence of the free surface is thereby taken into account. To determine the extent of the validity of this analogy additional experimental work was carried out on flat plates with the same profile area and geometry as those of the corresponding hull-skeg configurations. The computed lift and yawing moment coefficients are compared in the present report with existing low aspect ratio wing theories, and results of these comparisons reveal the validity of the above analogy.

Finally an evaluation of the possible use of the flat-plate analogy is undertaken to determine if the stability indices can be obtained with accuracy by using the plate coefficients in lieu of those of the hull-skeg configurations. This substitution is found to be inadequate and the reasons for its failure are given.

In summary, the investigation described herein is divided into two parts: the first dealing with experimentation on the ship model fitted with various skegs, and the second with experimental work conducted on the flat-plate configurations.

In the first part, the static and dynamic coefficients for the lateral forces and moments obtained from straight-course experiments as well as by rotating-arm facilities are presented. Static force and moment coefficients obtained by interpolating the rotating-arm tests are compared with those obtained in the straight-course experiments.

The second part contains the experimental results obtained with the flat-plate configurations. A graphical comparison of these data with existing low aspect ratio wing theories is shown and results of the stability analysis described above are presented.

This study has been carried out at the Davidson Laboratory (formerly the Experimental Towing Tank), Stevens Institute of Technology, supported by the Bureau of Ships' Fundamental Hydromechanics Research Program, under Contract Nonr 263(16) and technically administrated by the David Taylor Model Basin (DL Project JU 2026).

NOMENCLATURE

A	Profile area of various configurations, in square feet, or as otherwise defined in the text
$\bar{c}$	Distance of the C.G. of the model from the tow point, in feet
AR	Geometric aspect ratio, H^2/A
B	Breadth of hull, in feet
C.G.	Center of gravity of various configurations
C_L	Lift coefficient
C_m	Moment coefficient
H	Draft of hull, in feet
h	Maximum height of various skegs
I_z	Moment of inertia of the hull about the z-axis
K	Radius of gyration of the hull about the z-axis
k	Coefficient expressing the ratio of experimental lift derivative to corresponding one of linear low aspect ratio theory (in terms of effective aspect ratio)
k_1, k_2, k'	Longitudinal, lateral and rotational (about z-axis) coefficients of accession to inertia, respectively
L	Length of hull, in feet (load waterline length)
ℓ	Length of skeg, in inches
M_o	Mass of various hull configurations, in slugs
M'_c	Mass of various plate configurations, in slugs
m'_1, m'_2	Longitudinal and lateral mass coefficients, respectively
N	Yawing moment, in lb.-ft.
N'	Yawing moment coefficient
N'_β, N'_r	Static and dynamic yawing moment derivative coefficients, respectively
N'_{β_i}	Yawing moment derivative coefficient in ideal fluid
n'_z	Moment of inertia coefficient about the z-axis
P	Profile area of various skegs, in square feet

P.H.,P.A.	Various plate configurations, where the latter "P" stands for plate and the remainder denotes the corresponding hull-skeg configurations
R	Radius of turning circle, in feet
S.A.,S.B.	Various skeg configurations, where the latter "S" stands for skeg and the remainder denotes the various types of skegs
V	Velocity of advance, in feet per second
X,Y	Longitudinal and lateral force respectively, in pounds
X',Y'	Longitudinal and lateral force coefficients, respectively
Y'_β,Y'_r	Static and dynamic lateral force derivative coefficients respectively
β	Yaw angle
ρ	Mass density of water, in slugs
$\sigma_{1,2}$	Roots of the stability equation, (stability indices)

DESCRIPTION OF MODEL AND TEST EQUIPMENT

The model used in this investigation was ETT No. 842, of the Taylor Standard Series, with all deadwood removed. Five configurations were tested: a bare hull and this hull fitted with four different skegs varying in size and position. Figure A-1 in Appendix A (page 62) shows a schematic drawing of the bare-hull model and the various appendages. The characteristic dimensions of model and appendages are given below.

PARTICULARS OF ETT MODEL 842 AND APPENDAGES

Model Particulars

Length, L, ft.	6.00
Breadth, B, ft.	0.870
Draft, H, ft.	0.298
Length-Beam ratio, L/B	6.90
Length-Draft ratio, L/H	20.1
Beam-Draft ratio, B/H	2.92
Weight, lbs.	48.40
Profile area, A, in square feet	1.534
Position of C.G. from bow, inches	37.44

Skeg Particulars

Skegs	max. ℓ inches	max. h inches	Area, P ft.^{2}	$\frac{P}{A}$%	C.G. of skeg from C.G. of hull, inches
S.A.	23.54	3.57	0.253	16.5	-27.15
S.B.	16.33	2.21	0.115	7.5	-22.27
S.C.	12.73	1.68	0.066	4.3	-19.82
S.D.	9	1.84	0.116	7.6	+27.45

The plus (+) and minus (-) signs indicate that the C.G. of the skeg lies fore (+) or aft (-) of the bare-hull C.G.

The thin plates used in the second part of the testing program were 1/8-inch aluminum alloy and had the same profile area and shape as the corresponding model configurations fitted with the various skegs, or bare. The following table gives the particulars of the plate models, designated by P.H., P.A., etc., where the first letter denotes the plate and the second the corresponding hull, i.e., "H" stands for bare-hull profile, "A" for hull plus skeg A, etc.

PARTICULARS OF PLATES CORRESPONDING TO THE MODEL
WITH VARIOUS APPENDAGES

Plate Configurations	Area, ft.^{2}	Weight, pounds	C.G. fwd of Tow point, ft.	Geometric Aspect Ratio
P.H.	1.534	9.68	0.335	0.0579
P.A.	1.787	10.11	0.223	0.0497
P.B.	1.649	9.82	0.297	0.0539
P.C.	1.600	9.73	0.313	0.0555
P.D.	1.650	9.89	0.386	0.0538

Tests were conducted using the rotating-arm in DL Tank No. 2 where the model was constrained to move in a circular path having a 32-foot radius, and in DL Tank No. 3 for the straight-course motion.

In the rotating-arm tests, the model was attached to a "balance beam" on the arm by means of a sloping plate having light flexures at each end connecting to the beam end to the deck of the model. The deflection of the balance beam (torque tube) which was attached to the rotating-arm by a spring, measured the longitudinal and transverse forces acting on the model and the yawing moments. The deflections were transformed into electrical signals which were transmitted to an electric meter "eshora". A Sanborn "150" Series oscillograph was used to measure the transmitted outputs.

The straight-course experiments were conducted in Tank No. 3, using the same towing system and measuring devices so that additional errors attributable to inconsistent mechanisms would be avoided. Thus, the straight-course data were obtained with the same degree of accuracy as the rotating-arm data.

The experiments were conducted at zero heel angle by restraining the torque tube and flexural plates in rolling motion.

A strut of 0.09 inch placed at an angle 20 degrees to the vertical and at a distance four inches in front of the bow (at water surface) was used as a turbulence stimulator throughout the experimental work.

General views of the model and plate configurations with the towing apparatus are given in Fig. A-2 and A-3 in Appendix A.

TEST PROGRAM AND PROCEDURE

The speed-length ratio, $V/\sqrt{L}$, was held fixed at a value of 0.8 throughout the investigation, while the experiments were conducted at the following yaw angles:

$$\beta = 0^\circ, \pm 2^\circ, \pm 4^\circ, \pm 6^\circ, \pm 10^\circ, \pm 14^\circ .$$

The rotating-arm tests were run with a 32-foot radius of turn. The model was set at a desired yaw angle and at zero heel angle throughout the experimentation.

The rotating-arm provides means for measuring forces and moments acting on a turning model at various radii, as well as speeds and yaw angles. However, in the present investigation only the maximum permissible turning radius was used because one objective was to show that hydrodynamic coefficients can be obtained by considering straight-course motion as an intermediate between a large turn to the right and a large turn to the left. The range of yaw angle, i.e., $-14^\circ \leq \beta \leq 14^\circ$, used throughout this investigation is the range of the linear behavior of hydrodynamic characteristics.

In this general setup, two forces, one along and the other perpendicular to the longitudinal plane of symmetry of the ship, were measured together with the yawing moments.

PRESENTATION AND DISCUSSION OF DATA

The test results obtained from this investigation are presented in Fig. 1 to 22.[a] These results are divided into two parts, one referring to the model-skeg configurations and the other to the flat-plate experiments.

For ease in working with the data, Table I lists the information given in each figure.

TABLE I

FIGURE INFORMATION

Configuration	Figure No.	Information
I : Model with various skegs	1 - 5	Y' , N'
	6 - 10	Comparison of rotating-arm data with straight-course experiments
	11	X'
II: Flat-plate configuration	12 - 16	Y' , N'
	17 - 21	Comparison of rotating-arm data with straight-course experiments
	22	X'
I + II	23 - 24	Y' and N' vs. β at r' = 0
I + II	25 - 26	Y' and N' vs. β at r' = 0.1875
I + II	27	Stability coefficients and hydrodynamic coefficients vs. profile area
I + II	28 - 29	Graphical comparison of experimental lift coefficients with that of low aspect ratio theories for various ship and plate configurations
I + II	30	Apparent center of pressure and probable true center of pressure
I + II	31	Ratio of experimental lift derivative coefficient to corresponding coefficient of the linear low aspect ratio theory vs. effective aspect ratio

The force data have been corrected for inertia and strut force. (See Tables IV and V on pages 22 to 29) The yawing moment coefficients of the models are as measured since the point of attachment (tow point) of the flexural plates and balance beam was vertically in line with the longitudinal

[a]All figures are numbered consecutively starting on page 31.

position of the model C.G. However, in the case of the flat-plate experiments, where the tow point was not in alignment with the vertical line through the plate C.G., a correction had to be made.

The following general formulas have been used for the hydrodynamic coefficients:

$$X' = \frac{X}{\frac{1}{2}\rho A V^2} + \frac{M_o(1 + k_2)}{\frac{1}{2}\rho A}\frac{\sin\beta}{R} \quad , \qquad (1)$$

$$Y' = \frac{Y}{\frac{1}{2}\rho A V^2} + \frac{M_o(1 + k_1)}{\frac{1}{2}\rho A}\frac{\cos\beta}{R} \quad , \qquad (2)$$

and

$$N' = \frac{N}{\frac{1}{2}\rho A L V^2} + \frac{M_o'(1 + k')}{\frac{1}{2}\rho A L}\frac{\cos\beta}{R}\bar{e} \quad , \qquad (3)$$

where

- X, Y, N = the measured forces (longitudinal and lateral) and yawing moment, respectively,
- M_o = mass of the hull configurations. M_o is kept constant in the case of the model-skeg configurations,
- M_o' = mass of the various plate configurations M_o' varies from configuration to configuration,
- k_1, k_2, k' = longitudinal, lateral and rotational (about z-axis) coefficients of accession to inertia, respectively,
- ρ = mass density of water, 1.937 slugs,
- β = yaw angle,
- R = radius of turning in feet,
- A = profile area of various configurations in square feet,
- $\bar{e}$ = distance of the C.G. of the model from the tow point. In the present case, $\bar{e}$ is positive, being located in front of the tow point,
- V = velocity, fps,
- L = length of configuration in feet,

The coefficients of accession to inertia have been considered to be equivalent to those given by Lamb[6] (page 155) for a prolate ellipsoid as a function of the ratio of minor to major axes. In this report the equiva-

lant form is considered to have as its major axis the ship length and as its minor axis twice the draft, i.e., twice the volume of the submerged part of the ship hull. In the present case the following values were used:

$$k_1 = 0.02$$

$$k_2 = 0.96$$

$$k' = 0.88$$

The data which have been corrected (see Table I) are presented as coefficients of

1. hydrodynamic longitudinal force, X'
2. hydrodynamic lateral force, Y'
3. hydrodynamic yawing moment, N'

plotted against yaw angle, β . (See Fig. 1 to 5 and 11 for ship-skeg configurations and 12 to 16 and 22 for the corresponding flat plates.)

By cross-plotting the rotating-arm data, the static lateral force and moment coefficients at $r' = 0$ are determined. The static and damping force and moment derivatives Y'_β , N'_β , Y'_r , and N'_r can be computed by cross-plotting the data at $r' = \beta = 0$. These are summarized in Table II on the following page.

The results of the straight-course experiments are graphically compared in Fig. 6 to 10 and 17 to 21 with those obtained by cross-plotting the rotating-arm data. The excellent agreement shown (for both model and flat-plate cases), between straight-course experiments and interpolations of the rotating-arm experiments, leads to the conclusion that straight-course motion can be considered as an intermediate between a large turn to the right and a large turn to the left. Therefore, the derivatives of the static hydrodynamic coefficients can be determined equally well by either rotating-arm or straight-course experiments.

TABLE II

HYDRODYNAMIC FORCE AND MOMENT DERIVATIVES

AT $r' = \beta = 0$

Case	Static Derivatives		Damping Derivatives	
	Y'_β	N'_β	Y'_r	N'_r
Bare Hull	+.226	+.156	-.032	-.044
Hull + S.A.	+.337	+.087	+.093	-.070
Hull + S.B.	+.283	+.135	+.031	-.056
Hull + S.C.	+.239	+.145	+.012	-.049
Hull + S.D.	+.516	+.261	-.158	-.080
Plates: P.H.	+.415	+.149	+.037	-.040
P.A.	+.484	+.112	+.107	-.056
P.B.	+.458	+.129	+.072	-.053
P.C.	+.430	+.143	+.064	-.042
P.D.	+.630	+.206	-.027	-.078

The results of an attempt to correlate the hydrodynamic behavior of the ship model with that of the flat plate having the same profile area and geometry are shown in Fig. 23 to 26, where the static and dynamic coefficients for lateral forces and yawing moments are graphically compared. It may be noted that the forces and moments obtained from the flat-plate experiments have the same general trend as those of the corresponding models, with the exception that the forces show considerable deviation in magnitude. This can be explained qualitatively, at least, by a study made by Crabtree[7] who found that the pressure distribution over a thin plate (less than 12% thickness chord ratio) at various incidences shows a pronounced suction peak near the leading edge with a subsequent steep adverse pressure gradient. This causes laminar boundary layer separation, since the particles near the region of suction peak do not acquire sufficient energy to overcome the large pressure gradient and the existing friction losses in the boundary layer. The size and form of the separation region or "bubble" has a considerable effect on the pressure distribution and hence on the lateral force.

The variation of the bubble formation with thickness ratio, incidence angle and local Reynolds number has been correlated[7] with the pressure distribtuion, and it was found that a short bubble has very little effect on the pressure distribution as compared to the long bubble. Furthermore, as the Reynolds number decreases for a given incidence or remains constant for increasing angle of incidence, the length of the bubble increases and, con-

sequently, the pressure distribution is affected considerably. It is clear therefore, that, before reaching any conclusion for the hydrodynamic behavior of the thin plate, a detailed investigation must be undertaken to study experimentally the lateral force variation with the Reynolds number, angle of attack and geometry of the leading edge.

The attractiveness of the idea of hydrodynamic similarity between flat plates and surface ships of the same profile area led to the investigation of the degree of applicability of such an analogy to the more practical problem of estimating the dynamic stability of a hull using only flat-plate data. An analysis of dynamic stability of the various hull configurations was therefore conducted, and stability indices were compared with those obtained by using the mass coefficients of the ship and the corresponding hydrodynamic coefficients of the plates.

Results of this analysis are presented in Table III on the following page and in Fig. 27 where the stability indices and static and dynamic derivative coefficients are plotted versus the corresponding profile area. Unfortunately this comparison shows that immediate practical use of this analogy is not possible as long as the lateral force on the plate behaves so capriciously compared to the lateral force exerted on the surface ship.

The dynamic stability indices for various hull and plate configurations have been calculated from the stability equation given by Davidson and Schiff[1] by means of

$$\sigma_{1,2} = \frac{\left[n_z'Y_\beta' - m_z'N_r'\right] \pm \left\{(n_z'Y_\beta' - m_2'N_r')^2 + 4m_2'n_z'\left[Y_\beta'N_r' + (m_1' - Y_r')N_\beta'\right]\right\}^{\frac{1}{2}}}{2m_2'n_z'} \qquad (4)$$

where all the symbols are according to the nomenclature adopted by the Society of Naval Architects and Marine Engineers.

Table III presents the mass $(m_1'\ ,\ m_2')$ and inertial (n_z') coefficients of the various configurations together with the stability indices.

In the non-dimensionalizing process for the mass coefficients $m_1'\ ,\ m_2'$ and inertia coefficient n_z' , the quantities $\frac{1}{2}\rho\ AL$ and $\frac{1}{2}\rho\ AL^3$ were respectively used. Furthermore, the moment of inertia of the hull about the z-axis is computed by means of the following expression:

$$I_z = M_o K^2 = M_o (\frac{L}{4})^2 \quad , \qquad (5)$$

where M_o = mass of the hull configuration,
K = radius of gyration,
L = load waterline length.

TABLE III

STABILITY INDICES

Case	Mass and Inertia Coefficients of Hull Configurations			Stability Indices - Mass and Hydrodynamic Coefficients of Ship Configurations		Stability Indices - Mass Coefficients Of Ship Configuration And Hydrodynamic Coefficients of Plates	
	m_1'	m_2'	n_z'	σ_1	σ_2	σ_1	σ_2
Bare Hull	.1723	.3304	.01987	+ .997	-3.876	+ .1196	-3.387
Hull + S.A.	.1479	.2836	.01705	- .907	-4.382	-1.261	-3.794
Hull + S.B.	.1604	.3075	.01849	+ .207	-4.208	- .564	-3.809
Hull + S.C.	.1652	.3167	.01905	+ .502	-3.823	- .1466	-3.378
Hull + S.D.	.1602	.3075	.01847	+1.024	-7.064	- .3392	-5.995

It is evident that all ship-skeg configurations are unstable except the one with the largest skeg, i.e., S.A. However, the hypothetical case, where mass and inertia coefficients of ship-skeg configurations were used together with the hydrodynamic coefficients of the corresponding plates, shows stability for all configurations. This, of course, is not surprising since, as has been mentioned before, the static and dynamic derivative coefficients of the lateral force on the plates are considerably greater than those of the corresponding hull configurations. (See Fig. 27)

In the final step of this investigation, correlation of the experimental results with the existing low aspect ratio wing theories was undertaken as another test of the validity of the hydrodynamic analogy between ship hulls and flat plates.

The comparison is limited to the following formulae of the low aspect ratio theories given by Flax and Lawrence[8].

Weinig: $C_L \cong \pi/2 \; AR \; \beta + 2\beta^2$ (6)

Scholz: $C_L \cong \pi/2 \; AR \; \beta + 3.6\beta^2$ (7)

Flax-Lawrence: $C_L \cong \pi/2 \; AR \; \beta + \beta^2$ (8)

Here the linear term is identical in all cases, whereas the quadratic term varies considerably depending upon the assumption made and -- in most in-

stances — upon the experiments taken into consideration. Scholz states that his empirical result is mostly applicable to flat plates of low aspect ratio. The Flax-Lawrence[8] formula is valid for $AR \leq 0.5$, where the cross-flow drag coefficient is taken to be unity. It must also be kept in mind that the shape of the leading edge is of utmost importance in selecting the quadratic term, since the formation of the bubble and its extent is greatly affected by the geometric condition of the leading edge. In the present investigation the rounded tip edge is considered in conformity with the model configuration.

An attempt to correlate the experimental results with the semi-empirical formula suggested by Whicker and Fehlner[9] showed a considerable discrepancy due to the fact that the non-linear effect was greatly exaggerated by the presence of the aspect ratio in the denominator. Presumably the authors introduced their formula on the assumption that the aspect ratio should be greater than unity, a fact which is valid for control surfaces.

The graphical comparison displayed in Fig. 28 for the lift coefficient shows that the Flax-Lawrence expression is in better agreement with the experiments conducted with the hull-skeg configuration, whereas the Scholz expression is in better agreement with the corresponding flat-plate experiments.

Another facet of this correlation is that aspect ratio variation does not explain the increment of lift coefficient developed on the hull-skeg configuration over the bare-hull case. Although the variation of aspect ratio does not actually produce an appreciable variation in the lift component of the various plate configurations (see Fig. 28), in the case of the hull-skeg configurations the same aspect ratio variation gives rise to a considerable increase in the corresponding lift coefficients. The exaggerated effect of the aspect ratio in the hull-skeg configuration may be attributed to the hull-skeg interference effects, which are believed to depend strongly upon the fullness of the ship. It is therefore plausible to conclude that the beam effect (fullness of the ship) is mainly responsible for the effectiveness of the skegs since the two other ship characteristics, namely draft and length, have already been taken into account, and moreover, since the addition of the same skeg area to the basic plate did not (as expected) increase the lift by any comparable amount. Before making use of the low aspect ratio theories, it seems of paramount importance to attempt to incorporate the beam effect in the expressions of these low aspect wing theories.

Furthermore, it is seen from Fig. 28 that the linear low aspect ratio theory is in agreement only with the bare-hull case around the neighborhood of $\beta = 0$. In Fig. 31 the ratio k of the slope of the experimental lift coefficient curve to the corresponding slope of the linear aspect ratio theory is plotted in terms of the aspect ratio, $AR = H^2/A$. The curves fitted by means of the least-square method show that the coefficient k varies linearly with the aspect ratio, AR, and its rate of change is more pronounced in the hull configuration than in the flat-plate cases. Furthermore, it was noticed that the value $k \sim 3$ for the plate A case, which actually corresponds to a rectangle, is very close to wind tunnel results for the same aspect ratio. (See Fig. 2 of Flax-Lawrence[8]) This fact indicates that the "solid wall" method employed in the present work in accounting for the free-surface effect is correct, and presumably excludes (for low Froude numbers) this effect as an attributable factor to the observed deviation between plate and corresponding hull configurations. From the previous discussion it is expected that k should not only be a function of AR but also a function of the fullness of the ship hull. Unfortunately, no conclusions or at least indications could be drawn from the available set of experiments since only two cases with variable beam ratios ($B/L \sim 0$ and 0.146) were considered.

An attempt was made also at correlating the measured moment coefficients with theory. Flax and Lawrence's empirical-theoretical formula for lift coefficient was multiplied by the distance of the apparent center of pressure from the C.G., i.e., dC_m/dC_L. This was obtained by dividing the experimentally obtained N'_β by L'_β, i.e., the moment coefficient derivative by the lift coefficient derivative. The dC_m/dC_L derived in this manner was found to be approximately constant over the yaw angle range for each configuration used. (See Fig. 30) The comparison of experimental and theoretical C_m is given on Fig. 29 for the bare hull, hull plus skeg A and flat plates "H" and "A" (using the Schole lift formula for the plates).

The apparent center of pressure, of course, disregards the existence of a pure couple acting on a body. A yawing couple would act on the body in an ideal fluid in the absence of lateral force. Following the simplified flow theory of Munk[10] and Albring[11] the moment coefficient could be expressed as

$$C_m = N'_\beta \beta = N'_{\beta_1} \beta + \frac{\ell_p}{L} \left(\frac{\pi}{2} AR \; \beta\right) \quad , \tag{9}$$

where N'_{β_i} is the destabilizing moment coefficient derivative in an ideal fluid, $(\pi/2 \, AR \, \beta)$ equals C_L in the linear low aspect ratio theory, and ℓ_p is the distance from the true center of pressure to the C.G. The lower part of Fig. 30 is a plot of experimental N'_β versus Y'_β at $\beta = 0$. Fitting the theoretical linear equation (see Munk[10] and Albring[11]),

$$N'_\beta = N'_{\beta_i} + \frac{\ell_p}{L} Y'_\beta \quad , \tag{10}$$

to the data points gives an indication of both the ideal moment rate N'_{β_i}, the ordinate intercept, and the actual center of pressure position, ℓ_p/L, the slope of the line. The values thus obtained are substituted in Eq. 9 and the moment coefficients, according to this foregoing simplified flow theory, are plotted in Fig. 29 with the other experimental and theoretical moment coefficients.

It is evident that the combination of the Flax-Lawrence formula with the apparent location of the center pressure (obtained from the experiments by means of dC_m/dC_L) gives satisfactory results when compared with those obtained by experiments with the various model configurations. In addition, Scholz' formula multiplied by the location of the apparent center of pressure, dC_m/dC_L, describes closely the plate configurations. If, however, more realistic procedure (simplified flow theory) is used for the determination of the location of the center of pressure, then the linear low aspect ratio expression well represents the bare-hull case and fairly well the plate-hull case.

CONCLUDING REMARKS AND RECOMMENDATIONS

On the basis of the foregoing study the following broad conclusions can be reached:

1. Entirely reliable static force moment coefficients for straight-course motion can be obtained from rotating-arm data.
2. The similarity of results obtained for the hull-skeg configurations and corresponding flat plates of the same profile and area strengthens the prevailing belief in the analogy of surface ships to low aspect ratio wings. In particular, comparison of the hydrodynamic behavior of surface ships and flat plates shows that the yawing moments are in good agreement both in general trend and in magnitude, whereas the lateral forces show agreement in trend but considerable deviation in magnitude.
3. Stability analyses based on the coefficients of the hull-skeg configurations with the hydrodynamic coefficients of the corresponding plates substituted for those of the hull-skeg arrangements indicate that no immediate practical use can be made of the similarity shown, as long as no correction for the magnitudes of the lateral force of the plate is provided. It is known that the capricious behavior of the lateral force exerted on a thin plate is mainly attributable to the laminar boundary separation near its leading edge. The correction, therefore, should be a function of the local Reynolds number (based on the displacement thickness), of the incidence angle, and of the leading edge geometry.
4. The comparison of the experimental results for the lift coefficient with available low aspect ratio wing theories is another indication of the existing analogy between surface ships and aerofoils of low aspect ratio. The Flax-Lawrence expression is in better agreement with the surface ship data where non-linear terms are not so pronounced, whereas the Schola expression is in better agreement with the flat-plate data.
5. In the case of the bare hull only, the linear low aspect ratio theory closely describes the variation of the lift coefficient with the aspect ratio when the yaw angle, β , is in the neighborhood of zero. In all the other cases a factor, k , linearly dependent on aspect ratio, AR , must be used in order to bring the linear theory into agreement with experimental results.
6. Comparison of the moment coefficients shows that the Flax-Lawrence formula on one hand and Schola' on the

other combined with the apparent location of the center pressure (dC_m/dC_L) gives satisfactory results compared with the model end plate configurations, respectively. If, however, a more realistic procedure, i.e., simplified flow theory (valid in the linear region only), is used for the location of the center of pressure, the low aspect ratio linear expression well represents the bare-hull case and fairly well the plate-hull case.

7. The failure of aspect ratio variation to account for the observed variation in lift coefficient from the bare-hull configuration to the hull-skeg combination is an important drawback to the use of current theoretical analogies. Any approach based on low aspect ratio is of limited use when the hull-skeg interference effect is not taken into account. Specifically, it is believed that the fullness of a ship form should be incorporated in expressions of low aspect ratio wing theories, so as to bring the aerodynamic analogy into better agreement with experimental results obtained on ship forms.

8. The agreement between the experimental results and those obtained in a wind tunnel indicates that the free-surface effect is well accounted for by the "solid wall" method and, therefore, such an effect is excluded as a possible factor which contributed to the observed discrepancies between flat plates and hull configurations.

The effect of fullness and beam-length ratio on the hydrodynamic coefficients requires a systematic study, particularly in regard to the effect of adding skegs. The additional forces and moments produced by the hull when skegs are added must be isolated by measuring the forces and moments on the skeg and hull separately.

More specifically it is recommended that experimental work similar to that of the present investigation be undertaken using a family of forms of progressively increasing beam-length ratios. The first member could be a plate of the same profile as all other members of the family. The last member should be a form similar to a Series 60 design. The effectiveness of adding a single skeg to each member could next be determined by separate determination of skeg and hull forces and moments.

Furthermore, the laminar separation "bubble" near the leading edge of the thin forms should be studied experimentally for moderate values of incidence to develop means of preventing the appearance of such zones of separation. If this could be accomplished it is anticipated that the flat-plate analogy would be enhanced.

Analytical study within the framework of the low aspect ratio theory should be undertaken, since the present investigation has shown the validity of the analogy of ship hulls and wings of low aspect ratio.

ACKNOWLEDGEMENTS

The author wishes to express his indebtedness to Dr. John Breslin for his constructive suggestions and to Miss Winnifred Jacobs for her assistance during the preparation of this report.

REFERENCES

1. Davidson, K.S., and Schiff, L.: "Turning and Course-Keeping Qualities", Trans. SNAME, Vol. 54, November 1946.

2. Okada, S.: "Investigation of the Effect of the Propeller Race upon the Performance of Rudders", Second Report, Hydrodynamic Research of Ship Rudders, Hitachi Shipbuilding and Engineering Co., January 1959.

3. Romahn, K., and Thieme, H.: "On the Choice of the Balancing Areas of Rudders in the Propeller Slip Stream", Schiffstechnick, No. 21, April 1957.

4. Fedyaevsky, K.K., and Sobolev, G.V.: "Application of the Results of Low-Aspect Wing Theory to the Solution of Some Steering Problems", Proceedings of Netherlands Ship Model Basin Symposium on the Behavior of Ships in a Seaway, Wangeningen, Netherlands, September 1957.

5. Inoue, S.: "On the Turning of Ships", Memoires of the Faculty of Engineering, Kyushu University, Vol. XVI, No. 2.

6. Lamb, H.: "Hydrodynamics", Dover Publications, Sixth Edition, New York, New York, 1945.

7. Crabtree, L.F.: "The Formation of Regions of Separated Flow on Wing Surfaces", Part II, Royal Aircraft Establishment, Report AERO. 2578, July 1957.

8. Flax, A.H., and Lawrence, H.R.: "The Aerodynamics of Low Aspect Ratio Wings and Wing Body Combinations", Published by the Royal Aeronautical Society, Third Anglo-American Aeronautical Conference, September 1951. Cornell Aeronautical Laboratory, Report 37, 1951.

9. Whicker, L.F., and Fehlner, L.F.: "Free-Stream Characteristics of a Family of Low Aspect Ratio, All-Movable Control Surfaces for Application to Ship Design", DTMB Report 933, December 1958.

10. Munk, M.M.: "Aerodynamic of Airships", Division Q, Section 9, Vol. VI of Aerodynamic Theory, Durand, W.F., editor, 1934.

11. Albring, W.: "Stability and Maneuverability of Bodies with Control Surfaces", Translation by Dr. Arthur Korn, ETT Note 38, April 1946.

TABLE IV

TABULATION OF MEASURED AND CORRECTED RESULTS FOR LONGITUDINAL, LATERAL FORCES AND YAWING MOMENTS

Turning Radius R = 32 feet

Model	β^{o}	Speed, V, fps	Measured X-Force lbs.	Measured Y-Force lbs.	Measured N-Moment lb.ft.	Corrected X-Force lbs.	Corrected Y-Force lbs.	Corrected N-Moment lb.ft.
Bare Hull	0	3.[illegible]6	-.2615	-.7101	-.8695	-.2615	-.0978	-.7749
	2	3.23	-.2712	-.5976	-.2670	-.2347	+.0031	-.1742
	4	3.34	-.3415	-.5334	+.2232	-.2634	+.1083	+.3225
	6	3.29	-.3636	-.3895	+.6687	-.2499	+.2305	+.7650
	10	3.29	-.4339	-.1277	+1.694	-.2445	+.4880	+1.791
	14	3.29	-.5226	+.2781	+3.077	-.2597	+.8862	+3.174
	- 2	3.32	-.2656	-.8772	-1.472	-.2336	-.2424	-1.374
	- 4	3.23	-.2096	-1.002	-2.008	-.2827	-.4026	-1.915
	- 6	3.26	-.2094	-1.216	-2.766	-.3210	-.6070	-2.671
	-10	3.29	-.1634	-1.850	-4.687	-.3527	-1.235	-4.591
	-14	3.32	-.0838	-2.560	-6.875	-.3515	-1.941	-6.777
	-14	3.29	-.0985	-2.598	-6.761	-.3614	-1.990	-6.665
Hull+Skeg A	0	3.38	-.2793	-.3500	-1.664	-.2793	+.3067	-1.563
	0	3.29	-.2878	-.3268	-1.558	-.2878	+.2965	-1.462
	2	3.26	-.3146	-.1265	-1.242	-.2774	+.4858	-1.147
	4	3.26	-.3455	+.1743	-1.157	-.2711	+.7856	-1.064
	6	3.29	-.3928	+.5345	-1.217	-.2792	+1.154	-1.121
	8	3.26	-.3912	+.9142	-1.191	-.2424	+1.521	-1.096
	10	3.29	-.4761	+1.342	-1.218	-.2867	+1.957	-1.122
	12	3.29	-.4718	+1.785	-1.201	-.2456	+2.398	-1.105
	14	3.29	-.5442	+2.315	-1.079	-.2813	+2.924	-.9814
	- 2	3.29	-.2380	-.4966	-2.153	-.2759	+.1266	-2.057
	- 4	3.32	-.1934	-.8485	-2.634	-.2711	-.2149	-2.536
	- 6	3.26	-.1664	-1.127	-3.146	-.2774	-.5177	-3.052
	-10	3.26	-.1254	-1.882	-4.465	-.3125	-1.277	-4.370
	-12	3.29	-.1353	-2.391	-5.345	-.3614	-1.779	-5.249
	-14	3.26	-.0670	-2.870	-6.059	-.3263	-2.273	-5.964
	-14	3.29	-.1028	-2.954	-6.265	-.3657	-2.346	-6.168
Hull+Skeg B	0	3.32	-.2513	-.5334	-1.223	-.2513	+.1014	-1.125
	2	3.32	-.2336	-.3802	-.8100	-.1951	+.2546	-.7119
	4	3.29	-.2607	-.1612	-.3798	-.1850	+.4609	-.2835
	6	3.29	-.2873	+.0801	-.1796	-.1742	+.7001	-.0833
	10	3.32	-.3956	+.6656	+.3394	-.2028	+1.293	+.4375
	14	3.29	-.4187	+1.397	+1.019	-.1547	+2.005	+1.116
	- 2	3.32	-.2116	-.6910	-1.862	-.2502	-.0562	-1.764
	- 4	3.26	-.1668	-.8961	-2.196	-.2393	-.3004	-2.104
	- 6	3.32	-.1840	-1.300	-3.108	-.2997	-.6689	-3.010
	-10	3.29	-.1353	-1.991	-4.512	-.3246	-1.375	-4.416
	-14	3.32	-.0804	-2.909	-6.392	-.3493	-2.290	-6.294

TABLE IV

CONTINUED

Model	β°	Speed, V, fps	Measured X-Force lbs.	Measured Y-Force lbs.	Measured N-Moment lb.ft.	Corrected X-Force lbs.	Corrected Y-Force lbs.	Corrected N-Moment lb.ft.
Hull+Skeg C	0	3.32	-.2502	-.5962	-1.041	-.2502	+.0386	-.9433
	2	3.35	-.2735	-.4708	-.4809	-.2343	+.1749	-.3811
	4	3.32	-.2281	-.2931	-.1598	-.1521	+.3405	-.0617
	6	3.29	-.2878	-.0866	+.1396	-.1742	+.5334	+.2359
	6	3.35	-.2825	-.1199	+.1199	-.1682	+.5224	+.2197
	10	3.35	-.3643	+.3924	+.8800	-.1682	+1.030	+.9798
	14	3.29	-.4458	+1.904	+1.742	-.1818	+2.512	+1.838
	-2	3.26	-.1658	-.6973	-1.648	-.2030	-.0850	-1.553
	-4	3.29	-.1710	-.9987	-2.218	-.2467	-.3765	-2.122
	-6	3.29	-.1396	-1.282	-2.986	-.2532	-.6622	-2.890
	-10	3.29	-.0995	-1.969	-4.631	-.2878	-1.354	-4.535
	-14	3.23	-.0719	-2.740	-6.28[illegible]	-.3261	-2.155	-6.191
Hull+Skeg D	0	3.29	-.2251	-1.136	-1.655	-.2251	-.5129	-1.559
	2	3.29	-.2597	-.7823	-.6600	-.2251	-.1591	-.5637
	4	3.32	-.2402	-.5235	+.1598	-.1697	+.1102	+.2579
	6	3.23	-.2553	-.2709	+.8388	-.1553	+.3261	+.9315
	10	3.32	-.3295	+.3350	+2.711	-.1532	+.9620	+2.809
	14	3.32	-.3582	+1.378	+5.312	-.1124	+1.997	+5.410
	-2	3.29	-.1872	-1.439	-2.608	-.2218	-.8158	-2.598
	-4	3.29	-.1363	-1.904	-4.133	-.2056	-1.282	-4.037
	-4	3.32	-.1719	-1.973	-4.199	-.2424	-1.339	-4.101
	-6	3.35	-.1906	-2.477	-5.527	-.2982	-1.835	-5.428
	-10	3.32	-.1333	-3.526	-8.541	-.3097	-2.899	-8.442
	-14	3.29	-.1125	-4.609	-11.74	-.3538	-4.001	-11.64
Plate "H"	0	3.32	-.0551	-.0981	-.8485	-.0551	-.1135	-.7152
	2	3.32	-.0452	+.1058	-.4507	-.0353	+.3174	-.3174
	4	3.32	-.0496	+.4121	-.1895	-.0242	+.6237	-.0562
	6	3.29	-.0801	+.7769	+.0995	-.0498	+.9835	+.2305
	10	3.29	-.0595	+1.818	+1.082	-.0087	+2.023	+1.213
	12	3.29	-.1298	+2.424	+1.872	-.0692	+2.629	+2.003
	14	3.32	-.1444	+3.306	+2.755	-.0672	+3.514	+2.887
	-2	3.32	-.0397	-.4077	-1.532	-.0496	-.1962	-1.398
	-4	3.29	-.0444	-.7466	-2.175	-.0682	-.5388	-2.044
	-6	3.29	-.0206	-1.244	-3.224	-.0498	-1.038	-3.093
	-10	3.32	-.0353	-2.457	-5.179	-.0860	-2.248	-5.046
	-14	3.32	-.0562	-3.934	-7.163	-.1278	-3.726	-7.031
Plate "A"	0	3.29	-.1104	+.1645	-1.353	-.1104	+.3765	-1.232
	2	3.29	-.0595	+.4350	-1.093	-.0487	+.6470	-.9727
	4	3.29	-.1050	+.8364	-.9835	-.0801	+1.047	-.8634
	6	3.29	-.0595	+1.369	-.9522	-.0281	+1.584	-.8321
	10	3.32	-.1245	+2.788	.5257	-.0716	+3.002	-.4033
	12	3.32	-.1201	+3.438	+.1047	-.0560	+3.652	+.2270
	14	3.26	-.1052	+3.859	+.5528	-.0298	+4.063	+.6697

TABLE IV

CONTINUED

Model	β°	Speed, V, fps	Measured X-Force lbs.	Measured Y-Force lbs.	Measured N-Moment lb.ft.	Corrected X-Force lbs.	Corrected Y-Force lbs.	Corrected N-Moment lb.ft.
Plate "A"	- 2	3.29	-.0649	-.1894	-2.099	-.0757	+.0227	-1.979
	- 4	3.36	-.0848	-.6565	-2.949	-.1107	-.4362	-2.824
	- 6	3.29	-.0595	-1.114	-3.452	-.0898	-.9013	-3.331
	- 8	3.29	-.0454	-1.639	-4.177	-.0876	-1.428	-4.056
	- 9	3.29	-.0747	-1.937	-4.642	-.1212	-1.726	-4.522
	-10	3.29	-.0649	-2.251	-5.280	-.1158	-2.041	-5.160
	-10	3.34	-.0747	-2.252	-5.765	-.1271	-2.036	-5.641
	-10	3.32	-.0937	-2.413	-5.620	-.1455	-2.200	-5.498
	-12	3.15	-.0500	-2.920	-5.800	-.1080	-2.726	-5.689
	-14	3.32	-.0595	-4.133	-6.645	-.1212	-3.920	-6.524
	-14	3.32	-.0551	-4.133	-6.667	-.1278	-3.920	-6.546
Plate "B"	0	3.29	-.0898	+.0249	-1.169	-.0898	+.2337	-1.041
	2	3.23	-.0855	+.2868	-.6988	-.0751	+.4881	-.5757
	4	3.29	-.0400	+.6708	-.6384	-.0151	+.8797	-.5118
	4	3.32	-.0595	+.6832	-.6061	-.0342	+.8959	-.4761
	6	3.32	-.0595	+1.102	-.4507	-.0287	+1.315	-.3207
	10	3.29	-.0898	+2.164	+.4891	-.0357	+2.372	+.6157
	10	3.32	-.1003	+2.226	+.3802	-.0474	+2.438	+.5091
	14	3.32	-.1047	+3.758	+1.741	-.0276	+3.967	+1.870
	- 2	3.32	-.0353	-.2942	-1.796	-.0309	-.0815	-1.730
	- 4	3.32	-.0694	-.8375	-2.645	-.0948	-.6248	-2.515
	- 6	3.32	-.0595	-1.311	-3.449	-.0904	-1.099	-3.318
	-10	3.32	-.0694	-2.535	-5.455	-.1212	-2.323	-5.326
	-14	3.29	-.0703	-4.058	-7.899	-.1407	-3.852	-7.772
Plate "C"	0	3.32	-.0804	-.0165	-.9312	-.0804	+.1962	-.8001
	2	3.32	-.0452	+.2215	-.5301	-.0353	+.4342	-.3989
	4	3.29	-.0400	+.5259	-.3603	-.0151	+.7347	-.2315
	6	3.32	-.0253	+1.014	-.1906	+.0055	+1.225	-.0595
	10	3.32	-.0452	+2.226	+.7648	+.0066	+2.437	+.8959
	14	3.32	-.0551	+3.626	+2.204	+.0220	+3.835	+2.334
	- 2	3.29	-.0400	-.3192	-1.612	-.0498	-.1104	-1.483
	- 4	3.26	-.0404	-.7898	-2.392	-.0648	-.5847	-2.265
	- 6	3.29	-.0303	-1.336	-3.246	-.0595	-1.129	-3.117
	-10	3.29	-.0454	-2.424	-5.334	-.0952	-2.217	-5.206
	-10	3.32	-.0595	-2.562	-5.444	-.1102	-2.345	-5.313
	-14	3.29	-.0303	-3.804	-6.665	-.0995	-3.787	-6.537
	-14	3.26	-.0446	-3.976	-7.111	-.1137	-3.774	-6.986
Plate "D"	0	3.29	-.0151	-.2867	-1.645	-.0151	-.0768	-1.507
	0	3.30	-.0195	-.2951	-1.714	-.0195	-.0846	-1.577
	2	3.30	-.0803	+.0488	-1.172	-.0694	+.2593	-1.034
	4	3.30	-.0998	+.3895	-.3396	-.0749	+.6000	-.2018

TABLE IV

CONTINUED

Model	β°	Speed, V, fps	Measured X-Force lbs.	Measured Y-Force lbs.	Measured N-Moment lb.ft.	Corrected X-Force lbs.	Corrected Y-Force lbs.	Corrected N-Moment lb.ft.
Piece "D"	6	3.30	-.0445	+.6705	+.4666	-.0130	+.8799	+.6033
	8	3.21	-.0453	+1.339	+1.272	-.0062	+1.538	+1.403
	10	3.18	-.0641	+1.837	+1.912	-.0160	+2.029	+2.038
	14	3.23	-.0604	+3.185	+3.716	-.0125	+3.384	+3.848
	- 2	3.18	-.0290	-.7157	-2.49[illegible]	.0390	-.5215	-2.365
	- 2	3.24	-.0347	-.7035	-2.562	-.0242	-.4998	-2.429
	- 4	3.23	-.0094	-1.161	-3.591	-.0333	-.9588	-3.459
	- 6	3.33	-.0599	-1.874	-4.846	-.0909	-1.660	-4.707
	-10	3.26	-.0553	-3.056	-7.452	-.1052	-2.852	-7.318
	-14	3.27	-.0203	-4.376	-9.940	-.0899	-4.172	-9.805

TABLE V

TABULATION OF MEASURED AND CORRECTED RESULTS FOR LONGITUDINAL, LATERAL FORCES AND YAWING MOMENTS

Straight Course r' = 0

Model	β^o	Speed, V, fps	Measured X-Force lbs.	Measured Y-Force lbs.	Measured N-Moment lb.ft.	Corrected X-Force lbs.	Corrected Y-Force lbs.	Corrected N-Moment lb.ft.
Bare Hull	0	3.24	-.368	0	-.0567	-.273	0	-.1145
	2	3.22	-.406	+.122	+.395	-.327	+.122	+.338
	4	3.24	-.683	+.284	+1.071	-.597	+.284	+1.013
	4	3.19	-.454	+.337	+1.122	-.371	+.337	+1.066
	6	3.23	-.636	+.441	+1.589	-.547	+.441	+1.532
	8	3.25	-.578	+.572	+2.247	-.577	+.572	+2.189
	10	3.20	-.561	+.755	+3.091	-.463	+.755	+3.035
	10	3.16	-.474	+.659	+3.006	-.378	+.659	+2.951
	12	3.26	-.637	+1.126	+3.887	-.530	+1.126	+3.829
	14	3.26	-.589	+1.380	+4.669	-.481	+1.380	+4.613
	14	3.21	-.425	+1.444	4.811	-.312	+1.444	+4.752
	14	3.16	-.499	+1.468	+4.683	-.344	+1.468	+4.629
	- 2	3.24	-.588	-.102	-.536	-.519	-.102	-.593
	- 4	3.23	-.595	-.267	-1.107	-.532	-.267	-1.163
	- 6	3.24	-.567	-.389	-1.659	-.508	-.389	-1.717
	-10	3.25	-.625	-.943	-3.180	-.577	-.943	-3.238
	-14	3.26	-.658	-1.604	-5.098	-.621	-1.604	-5.144
	-14	3.17	0	-1.658	-4.995	0	-1.658	-5.050
Hull+Skeg A	0	3.22	-.655	0	-.114	-.582	0	+.172
	2	3.20	-.581	+.224	+.270	-.504	+.224	+.214
	4	3.21	-.530	+.459	+.709	-.448	+.459	+.653
	6	3.20	-.602	+.663	+.908	-.514	+.663	+.852
	6	3.30	-.709	+.741	+1.036	-.615	+.741	+.976
	10	3.20	-.683	+1.377	+1.510	-.585	+1.377	+1.454
	10	3.31	-.682	+1.617	+1.782	-.576	+1.617	+1.722
	14	3.19	-.683	+2.346	+2.305	-.575	+2.346	+2.249
	14	3.19	-.683	+2.448	+2.407	-.575	+2.448	+2.351
	- 2	3.35	-.516	-.224	-.516	-.442	-.224	-.577
	- 6	3.20	-.632	-.571	-1.040	-.575	-.571	-1.097
	-10	3.20	-.643	-1.377	-1.907	-.596	-1.377	-1.964
	-10	3.35	-.617	-1.659	-2.051	-.571	-1.659	-2.113
	-14	3.35	-.527	-2.959	-3.072	-.486	-2.959	-3.133
Hull+Skeg B	0	3.37	-.536	-.0228	+.091	-.456	-.0228	+.0285
	2	3.38	-.559	+.182	+.570	-.472	+.182	+.507
	4	3.41	-.580	+.499	+1.056	-.486	+.499	+.992
	6	3.30	-.545	+.610	+1.428	-.451	+.610	+1.368
	10	3.31	-.550	+1.140	+2.230	-.454	+1.140	+2.175
	14	3.26	-.647	+2.332	+3.805	-.534	+2.332	+3.747
	- 2	3.30	-.719	-.251	+4.578	-.647	-.251	+3.979
	- 4	3.26	-.625	-.466	-.996	-.561	-.466	-1.055

TABLE V

CONTINUED

Model	β°	Speed, V, fps	Measured X-Force lbs.	Measured Y-Force lbs.	Measured N-Moment lb.ft.	Corrected X-Force lbs.	Corrected Y-Force lbs.	Corrected N-Moment lb.ft.
Hull+Skeg B	-10	3.30	-.447	-1.363	-2.572	-.397	-1.363	-2.632
	-14	3.28	-.659	-2.473	-3.877	-.621	-2.473	-3.915
Hull+Skeg C	0	3.35	-.381	0	-.056	-.303	0	-.118
	2	3.36	-.493	+.202	+.594	-.408	+.202	+.532
	4	3.34	-.526	+.459	+1.019	-.436	+.459	+.958
	4	3.29	-.464	+.421	+.994	-.377	+.421	+.934
	6	3.35	-.594	+.560	+1.568	-.497	+.560	+1.506
	10	3.36	-.583	+1.222	+2.892	-.475	+1.222	+2.831
	14	3.36	-.628	+2.242	+4.361	-.509	+2.242	+4.299
	- 2	3.36	-.617	-.202	-.594	-.543	-.202	-.656
	- 4	3.34	-.571	-.336	-1.098	-.503	-.336	-1.159
	- 6	3.28	-.535	-.524	-1.562	-.475	-.524	-1.621
	-10	3.26	-.541	-1.113	-2.756	-.492	-1.113	-2.814
	-14	3.27	-.599	-2.236	-4.408	-.562	-2.236	-4.467
Hull+Skeg D	0	3.24	-.503	-.096	-.171	-.428	-.096	-.230
	2	3.28	-.572	+.400	+.853	-.490	+.400	+.794
	4	3.26	-.604	+.784	+1.940	-.518	+.784	+1.882
	6	3.28	-.518	+1.145	+3.208	-.426	+1.145	+3.148
	10	3.32	-.594	+2.167	+5.500	-.488	+2.167	+5.440
	14	3.30	-.578	+3.074	+8.360	-.462	+3.074	+8.300
	- 2	3.30	-.643	-.349	-1.112	-.571	-.349	-1.172
	- 4	3.30	-.600	-.850	-2.278	-.533	-.850	-2.338
	- 6	3.28	-.464	-1.274	-3.456	-.404	-1.274	-3.515
	-10	3.28	-.583	-2.268	-5.962	-.534	-2.268	-6.021
	-14	3.28	-.670	-3.283	-8.651	-.632	-3.283	-8.710
Plate "H"	0	3.30	-.2834	-.0327	0	-.2071	-.0327	-.0600
	2	3.30	-.1744	+.2616	+.4251	-.0916	+.2616	+.3652
	4	3.28	-.3024	+.7452	+.9828	-.2149	+.7452	+.9234
	6	3.30	-.3161	+1.199	+1.700	-.2224	+1.199	+1.640
	8	3.22	0	+1.842	+2.484	0	+1.842	+2.427
	10	3.24	-.3045	+2.436	+3.308	-.2037	+2.436	+3.250
	10	3.24	-.2100	+2.226	+3.297	-.1092	+2.226	+3.239
	12	3.16	0	+2.540	+4.350	0	+2.540	+4.295
	14	3.24	0	+3.108	+5.355	0	+3.108	+5.297
	14	3.17	0	+3.454	+5.353	0	+3.454	+5.297
	14	3.28	-.2365	+3.859	+5.354	-.1226	+3.859	+5.294
	- 2	3.26	-.2014	-.2968	-.3922	-.1314	-.2968	-.4505
	- 4	3.30	-.2398	-.6976	-.9919	-.1733	-.6976	-1.052
	- 6	3.34	-.4256	-1.266	-1.613	-.3629	-1.266	-1.674
	-10	3.30	-.3161	-2.376	-3.183	-.2660	-2.376	-3.243
	-14	3.28	-.3010	-4.214	-6.773	-.2634	-4.214	-6.832
	-14	3.18	0	-3.366	-5.192	0	-3.366	-5.248

TABLE V

CONTINUED

Model	β°	Speed, V, fps	Measured X-Force lbs.	Measured Y-Force lbs.	Measured N-Moment lb.ft.	Corrected X-Force lbs.	Corrected Y-Force lbs.	Corrected N-Moment lb.ft.
Plate "A"	0	3.36	-.2486	0	-.0565	-.1695	0	-.1187
	2	3.37	-.2859	+.3311	+.2825	-.2000	+.3311	+.2203
	4	3.32	-.3333	+.8415	+.7051	-.2442	+.8415	+.6446
	6	3.30	-.3085	+1.297	+1.221	-.2147	+1.297	+1.161
	10	3.34	-.4301	+2.576	+2.520	-.3226	+2.576	+2.158
	14	3.32	-.4246	+4.345	+4.279	-.3080	+4.345	+4.219
	14	3.36	-.3447	+4.351	+3.978	-.2248	+4.351	+3.915
	14	3.32	-.3443	+4.345	+3.982	-.2277	+4.345	+3.922
	-2	3.32	-.3465	-.3234	-.4499	-.2739	-.3234	-.5104
	-4	3.32	-.3300	-.8745	-.9295	-.2629	-.8745	-.9900
	-6	3.29	-.2899	-1.286	-1.417	-.2289	-1.286	-1.477
	-10	3.24	-.3077	-2.594	-2.814	-.2594	-2.594	-2.872
	-14	3.26	-.2968	-4.081	-4.325	-.25[illegible]7	-4.081	-4.383
Plate "B"	0	3.38	-.1827	0	+.0343	-.1028	0	-.0286
	2	3.37	-.1596	+.3192	+.4560	-.0730	+.3192	+.3933
	4	3.37	-.2394	+.9006	+.9918	-.1471	+.9006	+.9291
	6	3.37	-.2166	+1.505	+1.562	-.1186	+1.505	+1.499
	6	3.21	-.2472	+1.164	+1.478	-.1586	+1.164	+1.421
	8	3.26	-.2024	+1.619	+2.194	-.1054	+1.619	+2.135
	8	3.28	0	+1.717	+2.333	0	+1.717	+2.273
	10	3.32	-.1998	+2.486	+2.964	-.0932	+2.486	+2.903
	12	3.19	0	+2.774	+3.662	0	+2.774	+3.606
	14	3.34	-.2464	+4.211	+4.906	-.1277	+4.211	+4.844
	-2	3.30	-.3815	-.2965	-.3728	-.3096	-.2965	-.4327
	-4	3.34	-.2800	-.8512	-.9106	-.2117	-.8512	-.9722
	-6	3.28	-.2376	-1.307	-1.501	-.1771	-1.307	-1.561
	-10	3.28	-.3888	-2.614	-3.143	-.3391	-2.614	-3.202
	-14	3.25	-.3074	-4.102	-4.908	-.2703	-4.102	-4.966
Plate "C"	0	3.30	-.1962	0	0	-.1853	0	-.0600
	2	3.30	-.2943	+.3161	+.4033	-.2115	+.3161	+.3434
	4	3.29	-.2170	+.8138	+.9982	-.1291	+.8138	+.9385
	6	3.30	-.2616	+1.286	+1.537	-.1679	+1.286	+1.477
	8	3.34	-.2352	+1.646	+2.386	-.1333	+1.646	+2.324
	8	3.32	-.2775	+2.198	+2.442	-.1765	+2.198	+2.381
	8	3.34	-.2464	+1.646	+2.307	-.1445	+1.646	+2.246
	8	3.39	-.2415	+1.829	+2.438	-.1369	+1.829	+2.375
	10	3.28	-.1935	+2.569	+3.236	-.0903	+2.569	+3.177
	10	3.37	-.1938	+2.645	+3.386	-.0844	+2.645	+3.323
	12	3.29	-.2705	+3.019	+4.025	-.1612	+3.019	+3.966
	14	3.22	-.2331	+4.040	+5.028	-.1154	+4.040	+4.967
	-2	3.36	-.1921	-.3164	-.4294	-.1175	-.3164	-.4916
	-4	3.36	-.1695	-.7345	-.8814	-.1006	-.7345	-.9436
	-6	3.36	-.2147	-1.254	-1.537	-.1514	-1.254	-1.599

TABLE V

CONTINUED

Model	β°	Speed.V. fps	Measured X-Force lbs.	Measured Y-Force lbs.	Measured N-Moment lb.ft.	Corrected X-Force lbs.	Corrected Y-Force lbs.	Corrected N-Moment lb.ft.
Plate "C"	- 8	3.39	-.1725	-1.725	-2.300	-.1139	-1.725	-2.363
	-10	3.36	-.2486	-2.735	-3.345	-.1966	-2.735	-3.407
	-14	3.38	-.2398	-4.248	-5.139	-.1999	-4.248	-5.202
Plate "D"	0	3.28	-.2808	+0.594	+0.842	-.2052	+.0594	+.0248
	2	3.31	-.3520	+.4620	+.0803	-.2684	+.4620	+.7425
	4	3.31	-.3080	+1.056	+1.760	-.2189	+1.056	+1.700
	4	3.26	-.2438	+.9010	+1.781	-.1579	+.9010	+1.723
	6	3.32	-.2886	+1.687	+2.786	-.1931	+1.687	+2.725
	10	3.32	-.2331	+2.964	+4.595	-.1265	+2.96[illegible]	+4.534
	10	3.32	-.1998	+3.075	+5.228	-.0932	+3.075	+5.167
	14	3.30	-.3052	+4.578	+7.783	-.1897	+4.578	+7.723
	14	3.30	-.2834	+4.251	+7.706	-.1679	+4.251	+7.646
	- 2	3.30	-.2289	-.3815	-.7630	-.1570	-.3815	-.8250
	- 4	3.31	-.1760	-.8030	-1.672	-.1089	-.8030	-1.733
	- 6	3.30	-.2289	-1.373	-2.747	-.1679	-1.373	-2.807
	-10	3.28	-.2484	-2.786	-5.054	-.1987	-2.786	-5.114
	-14	3.26	-.2226	-4.113	-9.116	-.1844	-4.113	-9.174

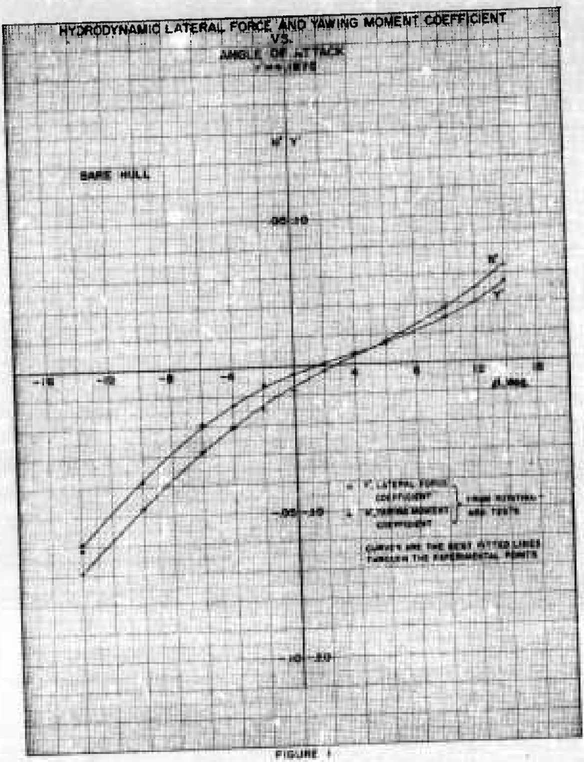
HYDRODYNAMIC LATERAL FORCE AND YAWING MOMENT COEFFICIENT
VS.
ANGLE OF ATTACK
BARE HULL

FIGURE 1

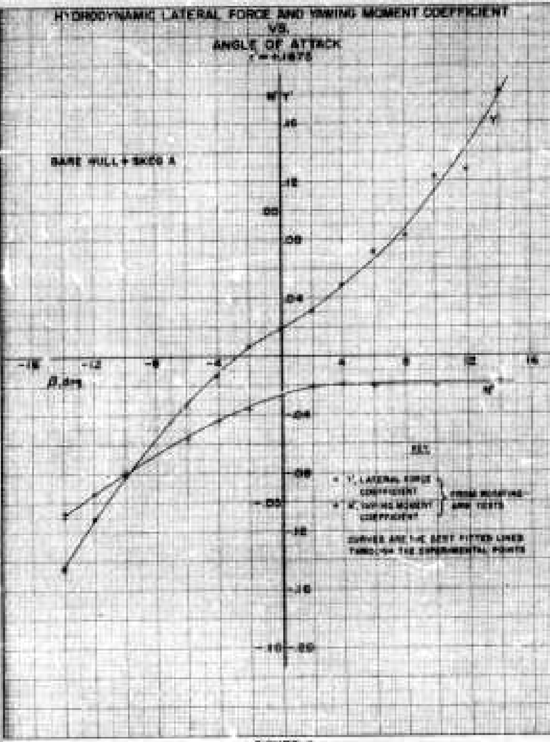
HYDRODYNAMIC LATERAL FORCE AND YAWING MOMENT COEFFICIENT
VS.
ANGLE OF ATTACK
BARE HULL + SKEG A
N', Y'
Y'
N'
β, deg
KEY
Y', LATERAL FORCE COEFFICIENT
N', YAWING MOMENT COEFFICIENT
FROM ROTATING ARM TESTS
CURVES ARE THE BEST FITTED LINES THROUGH THE EXPERIMENTAL POINTS

FIGURE 9

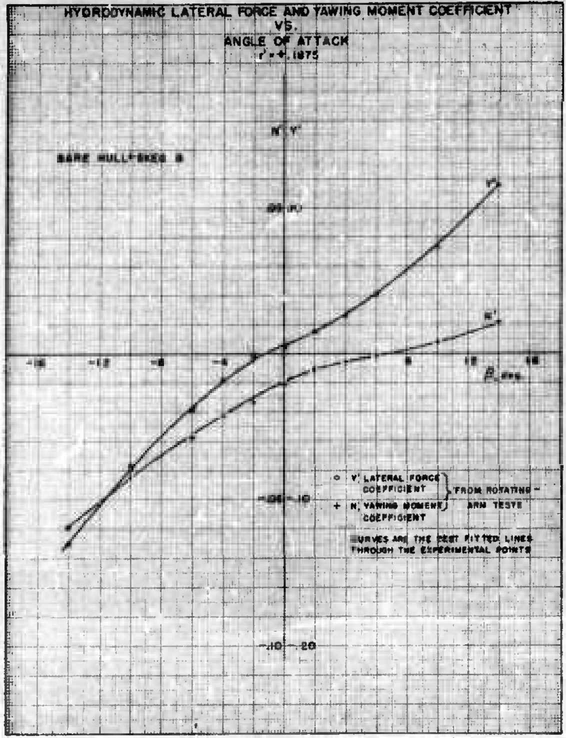
HYDRODYNAMIC LATERAL FORCE AND YAWING MOMENT COEFFICIENT
VS.
ANGLE OF ATTACK
r' = +.1875
N', Y'
BARE HULL-SKEG B
Y'
N'
β, deg.
○ Y' LATERAL FORCE COEFFICIENT
+ N' YAWING MOMENT COEFFICIENT
FROM ROTATING - ARM TESTS
CURVES ARE THE BEST FITTED LINES THROUGH THE EXPERIMENTAL POINTS

FIGURE 3

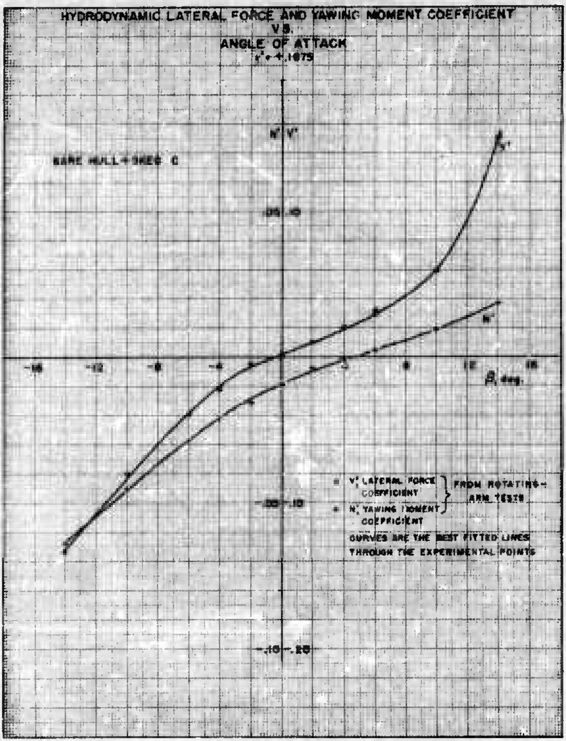
HYDRODYNAMIC LATERAL FORCE AND YAWING MOMENT COEFFICIENT
VS.
ANGLE OF ATTACK
BARE HULL + SKEG C
N' Y'
.05 .10
-.05 -.10
-.10 -.20
-16
-12
-8
-4
4
8
12
16
β, deg.
Y'
N'
Y', LATERAL FORCE COEFFICIENT
N', YAWING MOMENT COEFFICIENT
FROM ROTATING-ARM TESTS
CURVES ARE THE BEST FITTED LINES THROUGH THE EXPERIMENTAL POINTS

FIGURE 4

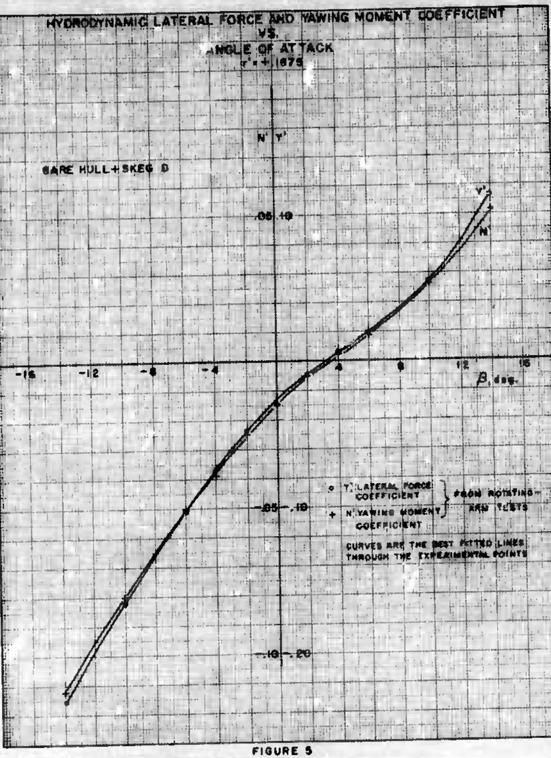
HYDRODYNAMIC LATERAL FORCE AND YAWING MOMENT COEFFICIENT
VS.
ANGLE OF ATTACK
BARE HULL + SKEG D
N' Y'
Y'
N'
.05 .10
-16
-12
-8
-4
4
8
12
16
β, deg.
-.05 -.10
-.10 -.20
o Y', LATERAL FORCE COEFFICIENT
+ N', YAWING MOMENT COEFFICIENT
FROM ROTATING-ARM TESTS
CURVES ARE THE BEST FITTED LINES THROUGH THE EXPERIMENTAL POINTS

FIGURE 5

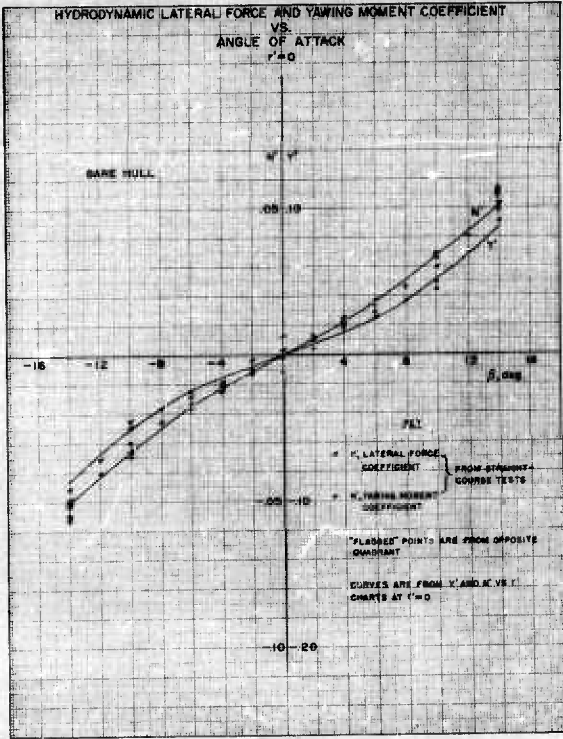
HYDRODYNAMIC LATERAL FORCE AND YAWING MOMENT COEFFICIENT
VS.
ANGLE OF ATTACK
r' = 0
BARE HULL
N', Y'
.05 .10
-16 -12 -8 -4 4 8 12 16
β, deg
N'
Y'
Y', LATERAL FORCE COEFFICIENT
N', YAWING MOMENT COEFFICIENT
FROM STRAIGHT-COURSE TESTS
-.05 -.10
"FLAGGED" POINTS ARE FROM OPPOSITE QUADRANT
CURVES ARE FROM Y' AND N' VS r' CHARTS AT r' = 0
-.10 -.20

FIGURE 6

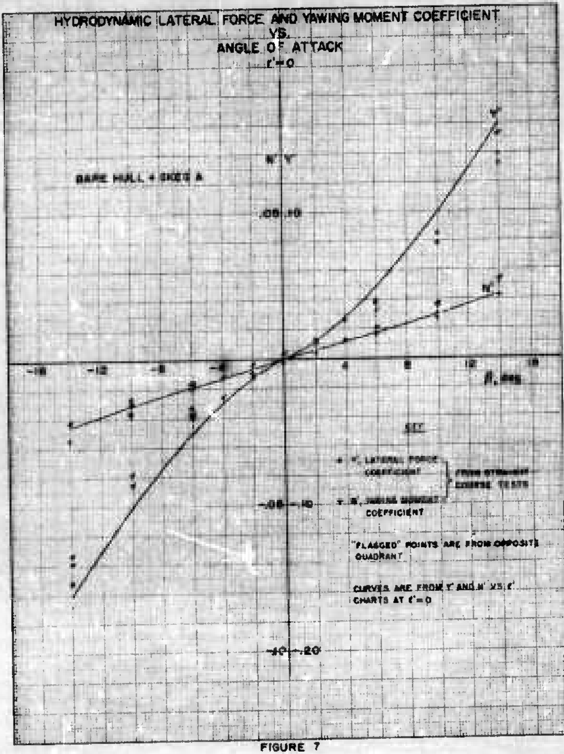
HYDRODYNAMIC LATERAL FORCE AND YAWING MOMENT COEFFICIENT
VS.
ANGLE OF ATTACK
r' = 0
BARE HULL + SKEG A
.05 .10
-.05 -.10
-.10 -.20
-16
-12
-8
-4
4
8
12
16
KEY
FLAGGED POINTS ARE FROM OPPOSITE QUADRANT
CURVES ARE FROM Y' AND N' VS r' CHARTS AT r' = 0

FIGURE 7

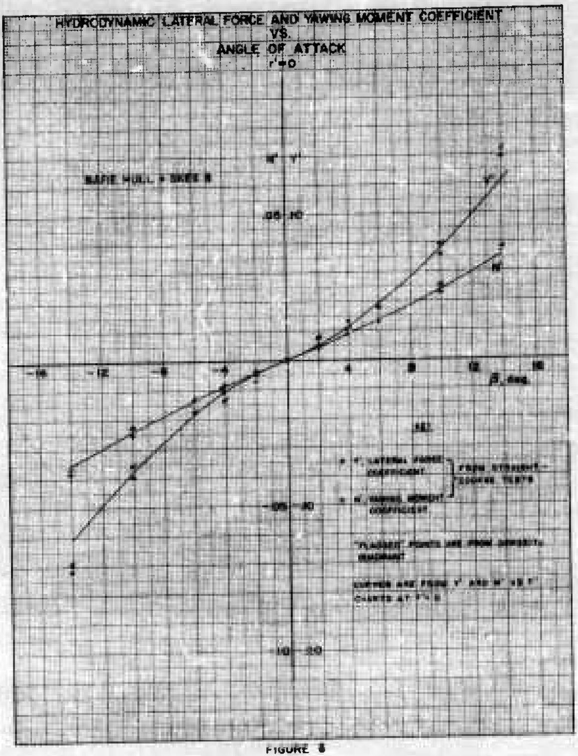
HYDRODYNAMIC LATERAL FORCE AND YAWING MOMENT COEFFICIENT
VS.
ANGLE OF ATTACK
r' = 0
N'
Y'
.05
.10
-.05
-.10
-.10
-.20
-16
-12
-8
-4
4
8
12
16
β, deg.

FIGURE

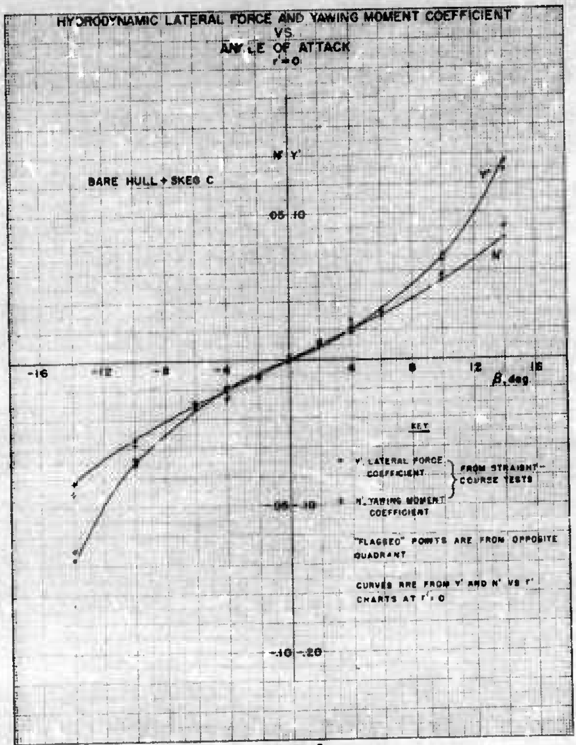
HYDRODYNAMIC LATERAL FORCE AND YAWING MOMENT COEFFICIENT
VS.
ANGLE OF ATTACK
r' = 0
BARE HULL + SKEG C
N' Y'
.05 .10
-.05 -.10
-.10 -.20
-16
-12
-8
-4
4
8
12
16
β, deg.
Y'
N'
KEY
Y', LATERAL FORCE COEFFICIENT
N', YAWING MOMENT COEFFICIENT
FROM STRAIGHT-COURSE TESTS
"FLAGGED" POINTS ARE FROM OPPOSITE QUADRANT
CURVES ARE FROM Y' AND N' VS r' CHARTS AT r' = 0

FIGURE 9

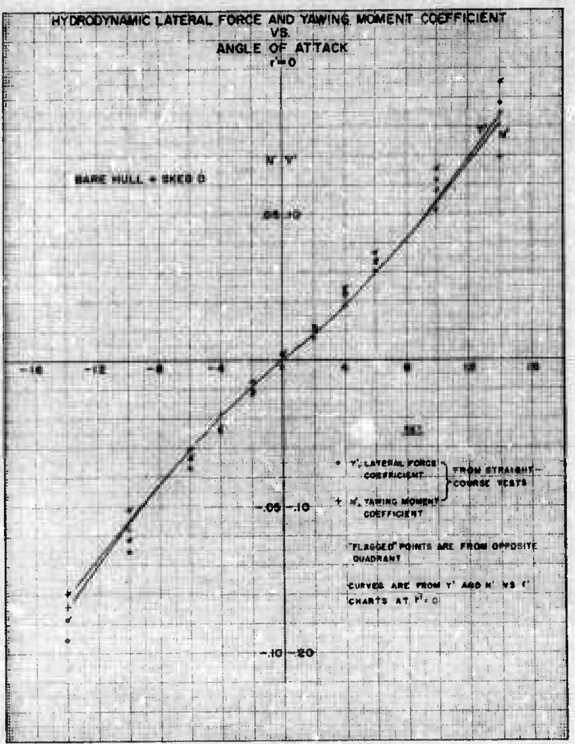
HYDRODYNAMIC LATERAL FORCE AND YAWING MOMENT COEFFICIENT
VS.
ANGLE OF ATTACK
r'=0
BARE HULL + SKEG D
N' Y'
.05 .10
-16
-12
-8
-4
4
8
12
16
-.05 -.10
-.10 -.20
Y', LATERAL FORCE COEFFICIENT
N', YAWING MOMENT COEFFICIENT
FROM STRAIGHT COURSE TESTS
"FLAGGED" POINTS ARE FROM OPPOSITE QUADRANT
CURVES ARE FROM Y' AND N' VS r' CHARTS AT r'=0

FIGURE 10

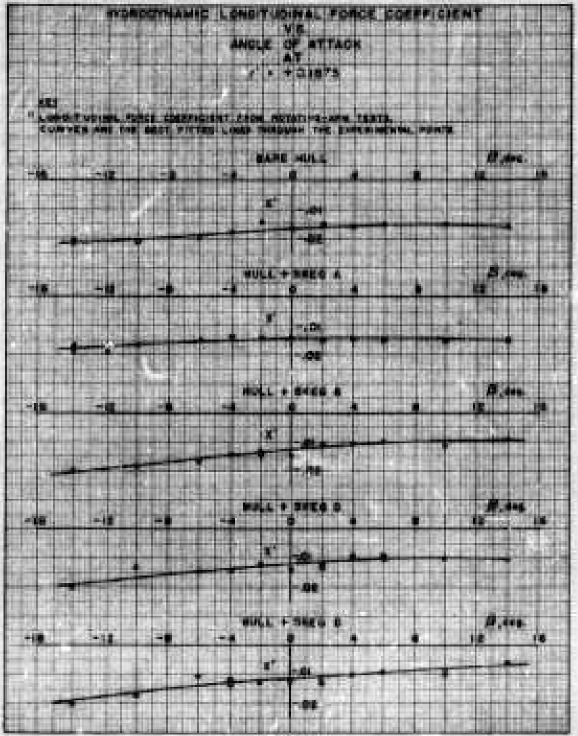
HYDRODYNAMIC LONGITUDINAL FORCE COEFFICIENT
VS
ANGLE OF ATTACK
AT
KEY
LONGITUDINAL FORCE COEFFICIENT FROM ROTATING-ARM TESTS
CURVES ARE THE BEST FITTED LINES THROUGH THE EXPERIMENTAL POINTS
BARE HULL
-16
-12
-8
-4
0
4
8
12
16
X'
HULL + SKEG A
HULL + SKEG B

FIGURE 11

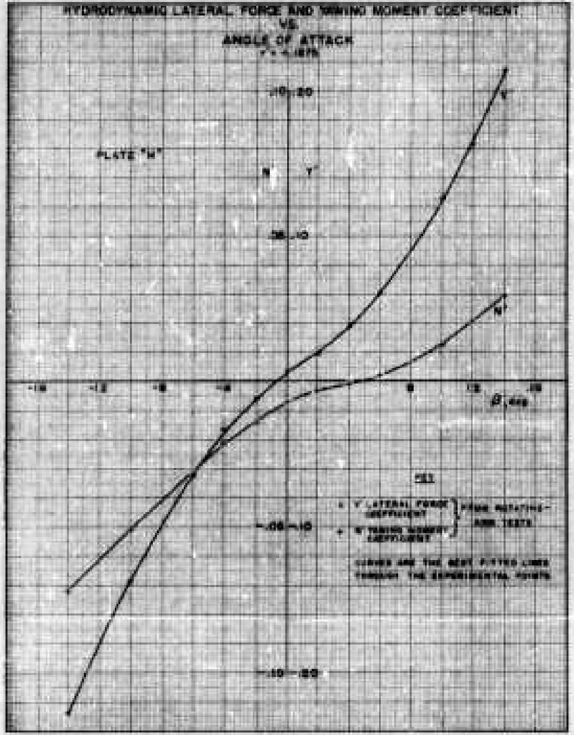
HYDRODYNAMIC LATERAL FORCE AND YAWING MOMENT COEFFICIENT
VS
ANGLE OF ATTACK
PLATE "H"
N' Y'
.10 .20
.05 .10
-.05 -.10
-.10 -.20
N'
Y'

FIGURE 12

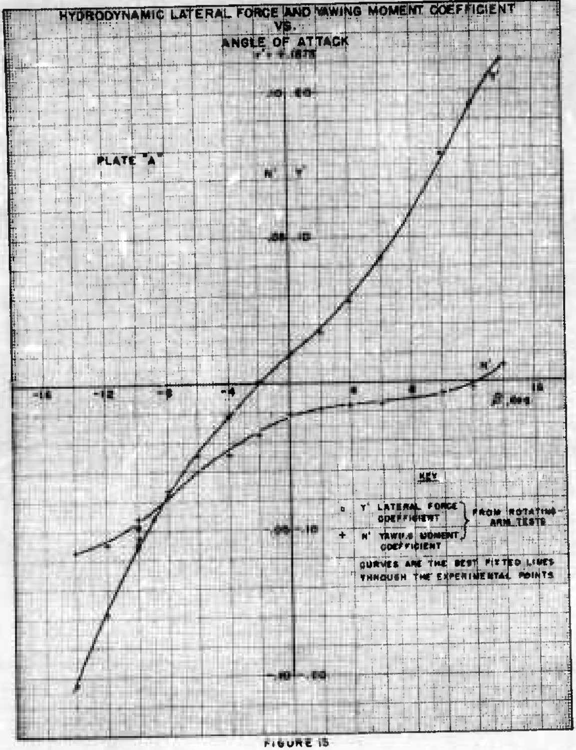
HYDRODYNAMIC LATERAL FORCE AND YAWING MOMENT COEFFICIENT
VS.
ANGLE OF ATTACK
PLATE "A"
N' Y'
KEY
Y' LATERAL FORCE COEFFICIENT
N' YAWING MOMENT COEFFICIENT
FROM ROTATING ARM TESTS
CURVES ARE THE BEST FITTED LINES THROUGH THE EXPERIMENTAL POINTS

FIGURE 15

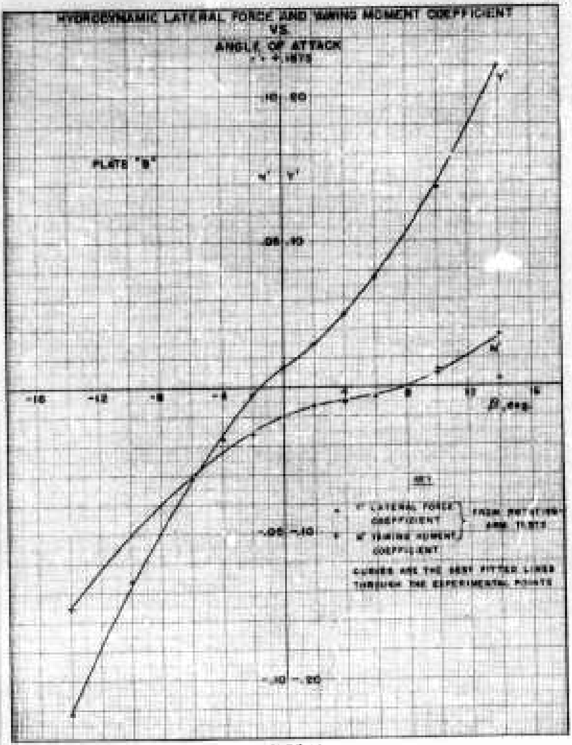
HYDRODYNAMIC LATERAL FORCE AND YAWING MOMENT COEFFICIENT
VS
ANGLE OF ATTACK
.10 .20
PLATE "B"
N' Y'
.05 .10
-16
-12
-8
-4
4
8
12
16
β, deg.
Y'
N'
KEY
Y' LATERAL FORCE COEFFICIENT
N' YAWING MOMENT COEFFICIENT
FROM ROTATING ARM TESTS
-.05 -.10
CURVES ARE THE BEST FITTED LINES THROUGH THE EXPERIMENTAL POINTS
-.10 -.20

FIGURE 14

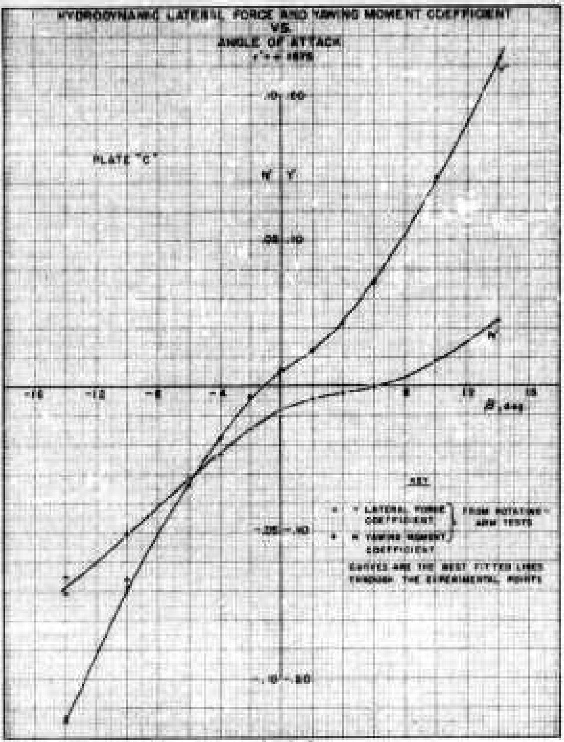

HYDRODYNAMIC LATERAL FORCE AND YAWING MOMENT COEFFICIENT
VS.
ANGLE OF ATTACK
PLATE "C"
N' Y'
β, deg
KEY
Y LATERAL FORCE COEFFICIENT
N YAWING MOMENT COEFFICIENT
FROM ROTATING-ARM TESTS
CURVES ARE THE BEST FITTED LINES THROUGH THE EXPERIMENTAL POINTS

FIGURE 15

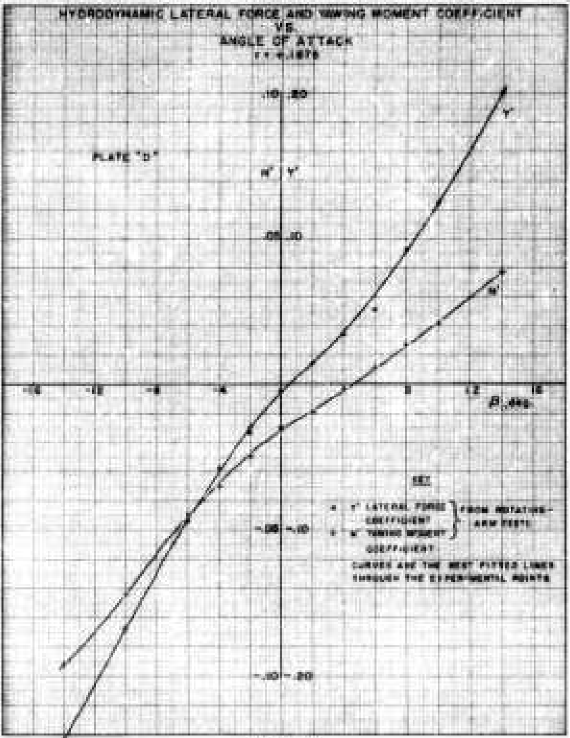
HYDRODYNAMIC LATERAL FORCE AND YAWING MOMENT COEFFICIENT
VS.
ANGLE OF ATTACK
.10 .20
PLATE "D"
N' Y'
Y'
.05 .10
N'
-16
-12
-8
-4
4
8
12
16
β, deg.
KEY
-.05 -.10
Y' LATERAL FORCE COEFFICIENT
N' YAWING MOMENT COEFFICIENT
FROM ROTATING-ARM TESTS
CURVES ARE THE BEST FITTED LINES THROUGH THE EXPERIMENTAL POINTS
-.10 -.20

FIGURE 16

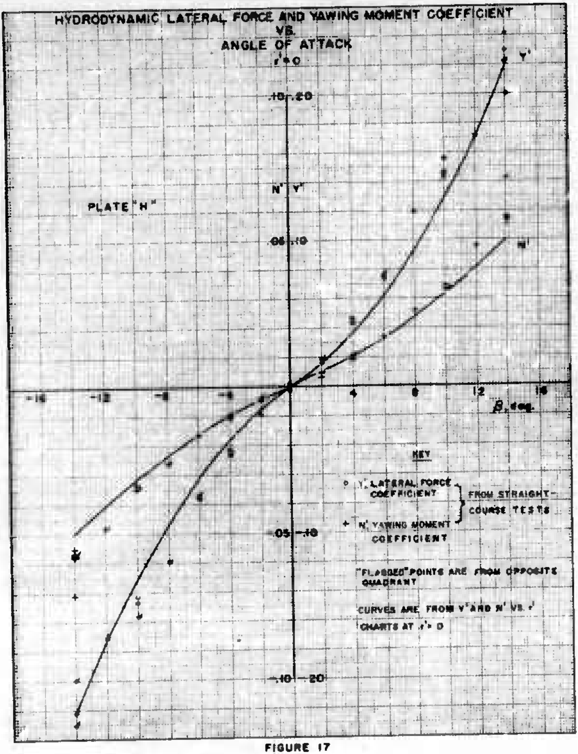
HYDRODYNAMIC LATERAL FORCE AND YAWING MOMENT COEFFICIENT
VS.
ANGLE OF ATTACK
r' = 0
PLATE "H"
N' Y'
.10 .20
.05 .10
-.05 -.10
-.10 -.20
-16
-12
-8
-4
4
8
12
16
β, deg.
Y'
N'
KEY
○ Y' LATERAL FORCE COEFFICIENT
+ N' YAWING MOMENT COEFFICIENT
FROM STRAIGHT-COURSE TESTS
"FLAGGED" POINTS ARE FROM OPPOSITE QUADRANT
CURVES ARE FROM Y' AND N' VS. r' CHARTS AT r' = 0

FIGURE 17

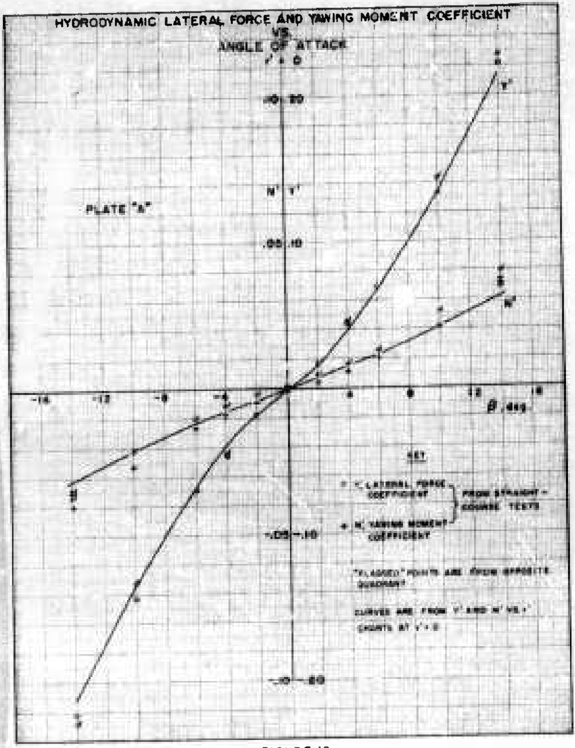
HYDRODYNAMIC LATERAL FORCE AND YAWING MOMENT COEFFICIENT
VS.
ANGLE OF ATTACK
N' Y'
.10 .20
.05 .10
-.05 -.10
-.10 -.20
-16
-12
-8
-4
4
8
12
16
β, deg.
Y'
N'

FIGURE 18

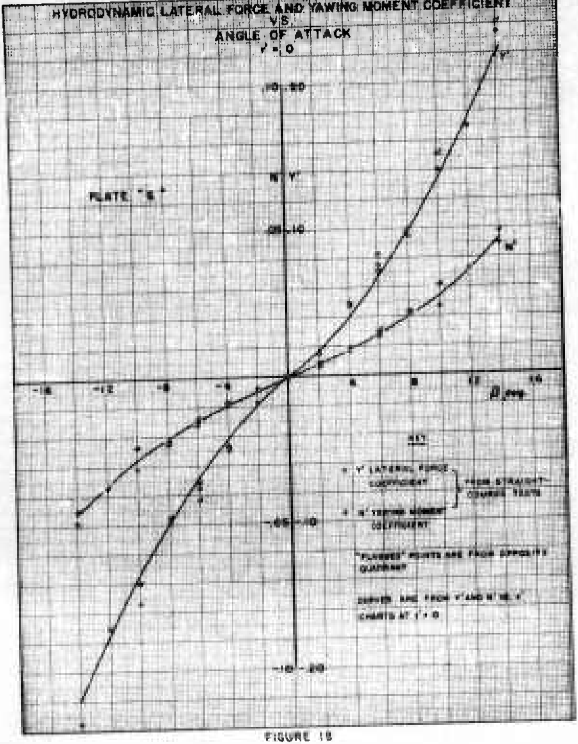
HYDRODYNAMIC LATERAL FORCE AND YAWING MOMENT COEFFICIENT
VS.
ANGLE OF ATTACK

FIGURE 15

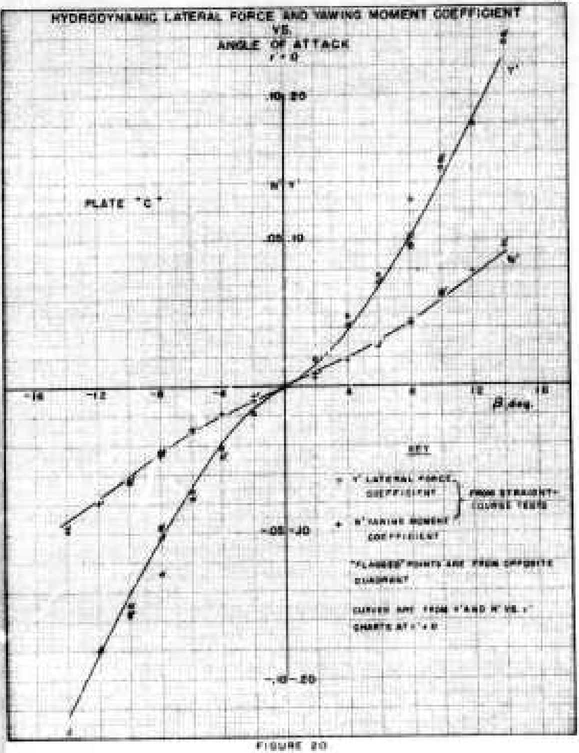
HYDRODYNAMIC LATERAL FORCE AND YAWING MOMENT COEFFICIENT
VS.
ANGLE OF ATTACK
r' = 0
PLATE "C"
N' Y'
.10 .20
.05 .10
-.05 -.10
-.10 -.20
-16
-12
-8
-4
4
8
12
16
β deg.
Y'
N'
KEY
Y' LATERAL FORCE COEFFICIENT
N' YAWING MOMENT COEFFICIENT
FROM STRAIGHT-COURSE TESTS
"FLAGGED" POINTS ARE FROM OPPOSITE QUADRANT
CURVES ARE FROM Y' AND N' VS. r' CHARTS AT r' = 0

FIGURE 20

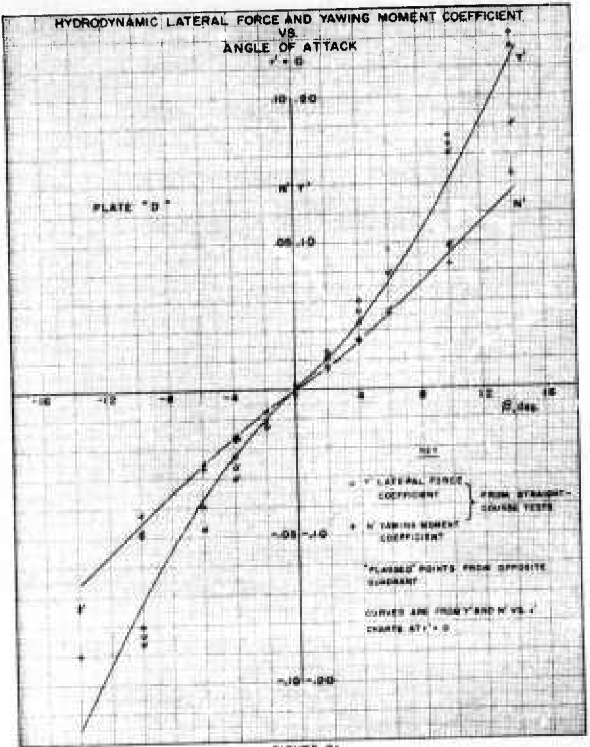
HYDRODYNAMIC LATERAL FORCE AND YAWING MOMENT COEFFICIENT
VS
ANGLE OF ATTACK
N' Y'
PLATE "D"
Y'
N'
.05 .10
-.05 -.10
-.10 -.20
.10 .20
LATERAL FORCE COEFFICIENT
YAWING MOMENT COEFFICIENT

FIGURE 21

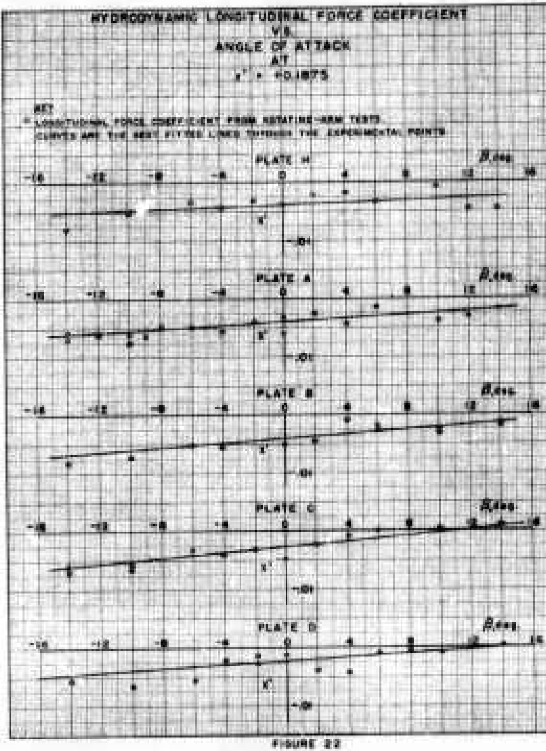
HYDRODYNAMIC LONGITUDINAL FORCE COEFFICIENT
VS.
ANGLE OF ATTACK
AT
PLATE H
PLATE A
PLATE B
PLATE C
PLATE D

FIGURE 22

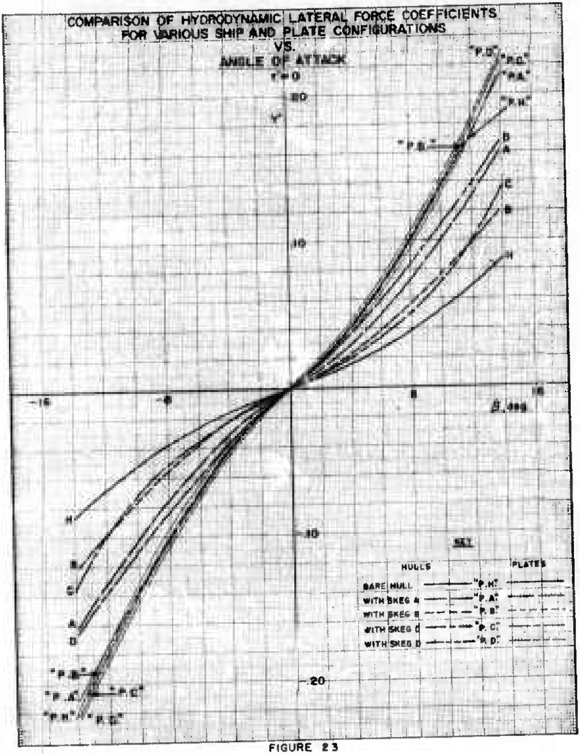
COMPARISON OF HYDRODYNAMIC LATERAL FORCE COEFFICIENTS
FOR VARIOUS SHIP AND PLATE CONFIGURATIONS
VS.
ANGLE OF ATTACK
HULLS
PLATES
BARE HULL
WITH SKEG A
WITH SKEG B
WITH SKEG C
WITH SKEG D
"P.H."
"P.A."
"P.B."
"P.C."
"P.D."
H
A
B
C
D
-15
-5
5
15
10
-10
-20

FIGURE 23

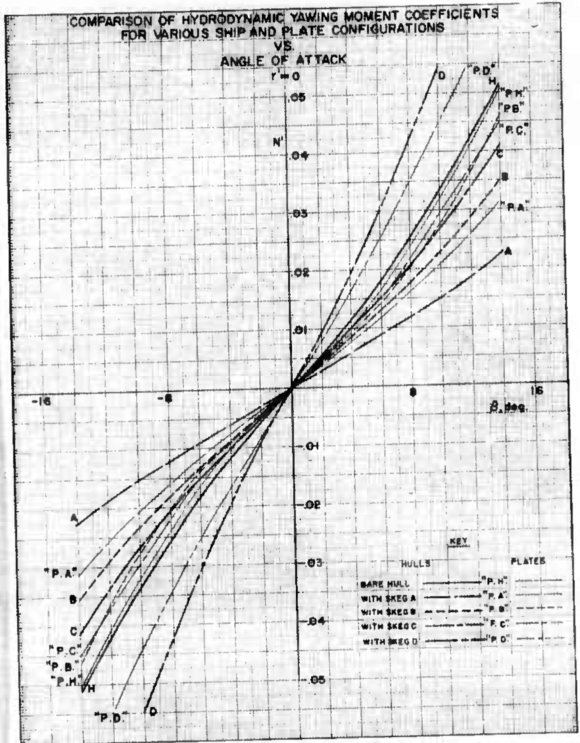
COMPARISON OF HYDRODYNAMIC YAWING MOMENT COEFFICIENTS
FOR VARIOUS SHIP AND PLATE CONFIGURATIONS
VS.
ANGLE OF ATTACK
r' = 0
N'
β, deg.
KEY
HULLS
PLATES
BARE HULL "P. H."
WITH SKEG A "P. A."
WITH SKEG B "P. B."
WITH SKEG C "P. C."
WITH SKEG D "P. D."

FIGURE 24

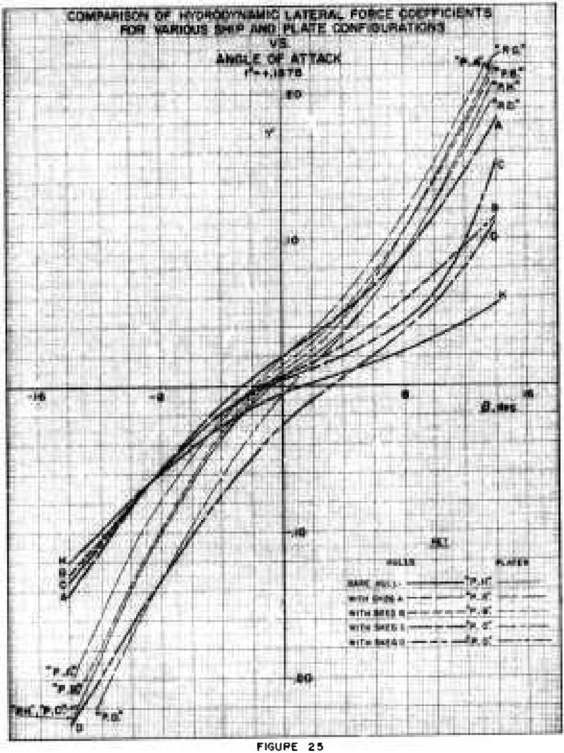
COMPARISON OF HYDRODYNAMIC LATERAL FORCE COEFFICIENTS
FOR VARIOUS SHIP AND PLATE CONFIGURATIONS
VS.
ANGLE OF ATTACK
20
10
-10
-20
-16
-8
8
16
HULLS
PLATES

FIGURE 25

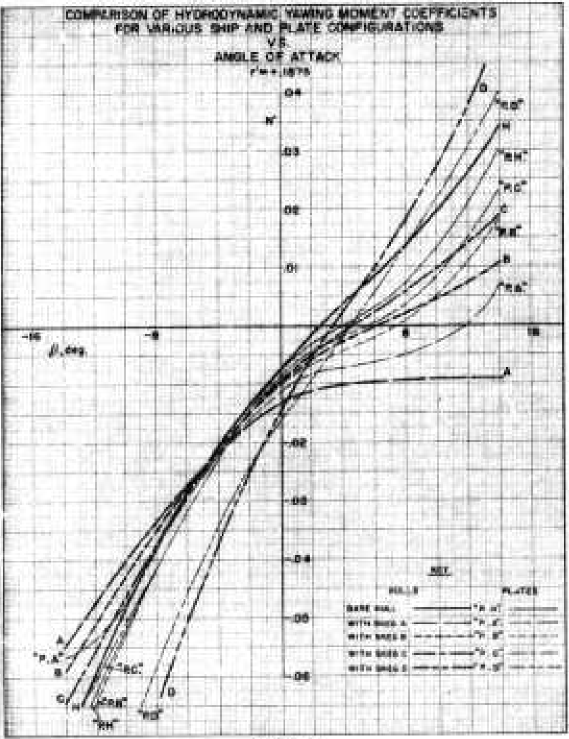

COMPARISON OF HYDRODYNAMIC YAWING MOMENT COEFFICIENTS
FOR VARIOUS SHIP AND PLATE CONFIGURATIONS
VS.
ANGLE OF ATTACK
N'
β, deg.
KEY
HULLS
PLATES
BARE HULL
WITH SKEG A
WITH SKEG B
WITH SKEG C
WITH SKEG D

FIGURE 26

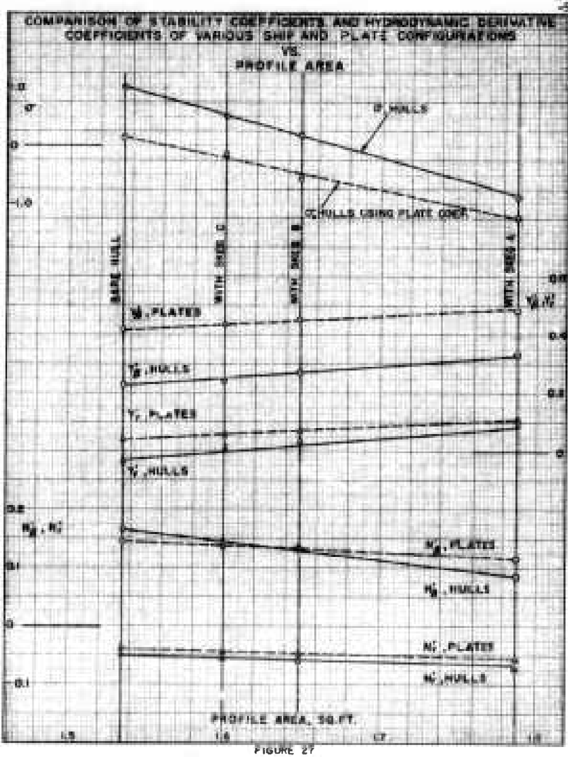

COMPARISON OF STABILITY COEFFICIENTS AND HYDRODYNAMIC DERIVATIVE COEFFICIENTS OF VARIOUS SHIP AND PLATE CONFIGURATIONS
VS.
PROFILE AREA
σ', HULLS
σ', HULLS USING PLATE COEF.
BARE HULL
WITH SKEG C
WITH SKEG B
WITH SKEG A
Y'_β, PLATES
Y'_β, HULLS
Y'_r, PLATES
Y'_r, HULLS
N'_β, N'_r
N'_β, PLATES
N'_β, HULLS
N'_r, PLATES
N'_r, HULLS
Y'_β, Y'_r
PROFILE AREA, SQ.FT.

FIGURE 27

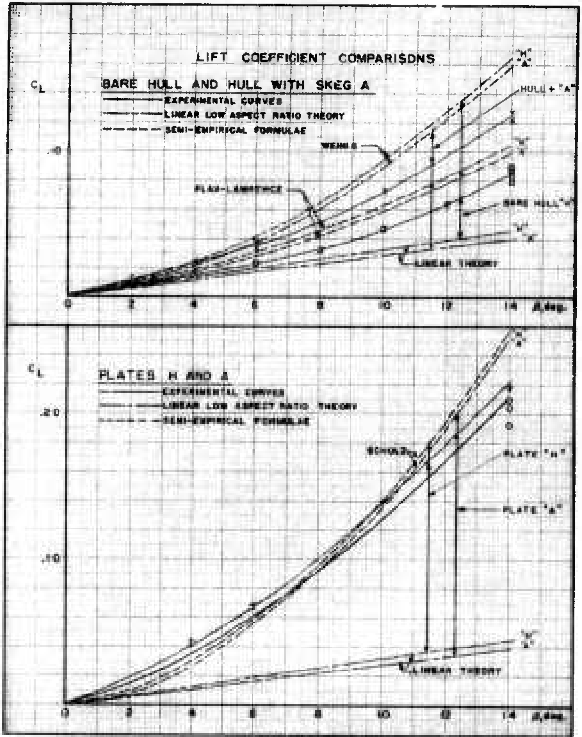
LIFT COEFFICIENT COMPARISONS
BARE HULL AND HULL WITH SKEG A
EXPERIMENTAL CURVES
LINEAR LOW ASPECT RATIO THEORY
SEMI-EMPIRICAL FORMULAE
HULL + "A"
BARE HULL "H"
LINEAR THEORY
PLATES H AND A
EXPERIMENTAL CURVES
LINEAR LOW ASPECT RATIO THEORY
SEMI-EMPIRICAL FORMULAE
PLATE "H"
PLATE "A"
LINEAR THEORY

FIGURE 29

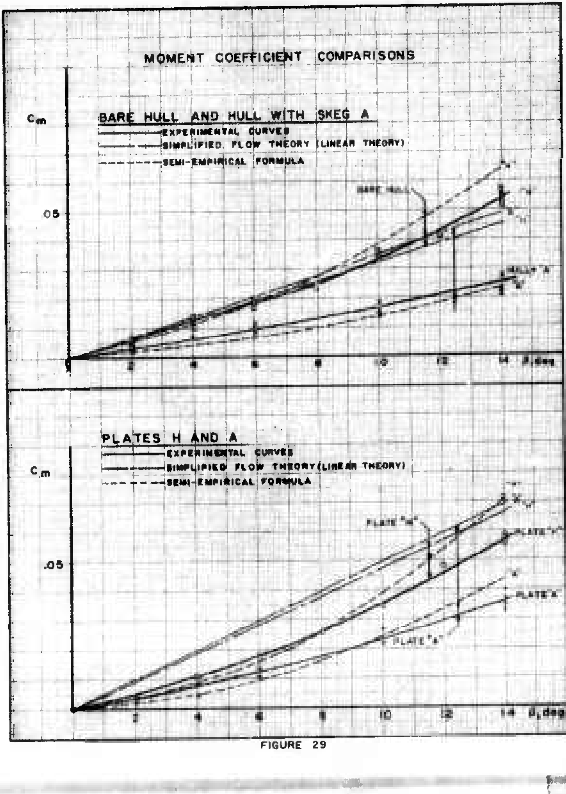
MOMENT COEFFICIENT COMPARISONS
BARE HULL AND HULL WITH SKEG A
EXPERIMENTAL CURVES
SIMPLIFIED FLOW THEORY (LINEAR THEORY)
SEMI-EMPIRICAL FORMULA
C_m
.05
BARE HULL
2
4
6
8
10
12
14
β, deg
PLATES H AND A
EXPERIMENTAL CURVES
SIMPLIFIED FLOW THEORY (LINEAR THEORY)
SEMI-EMPIRICAL FORMULA
C_m
.05
PLATE "H"
PLATE "A"
2
4
6
8
10
12
14
β, deg

FIGURE 29

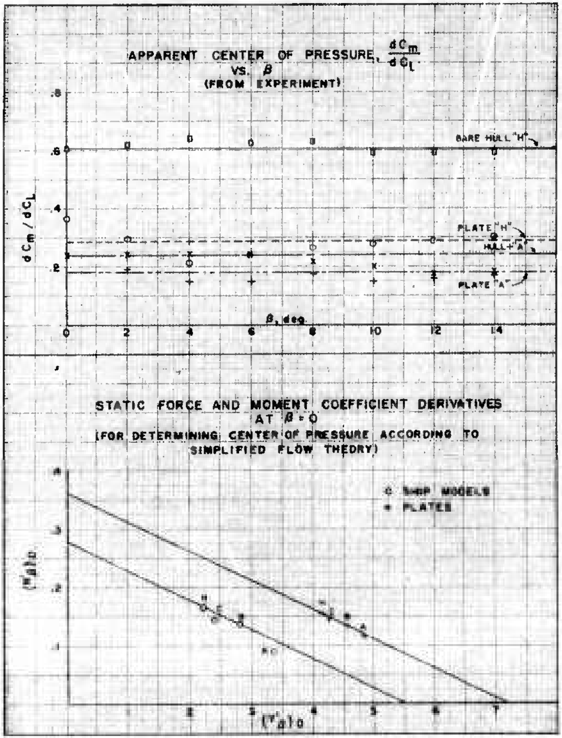
APPARENT CENTER OF PRESSURE, $\frac{dC_m}{dC_L}$ VS. β
(FROM EXPERIMENT)
dC_m / dC_L
BARE HULL "H"
PLATE "H"
HULL + "A"
PLATE "A"
β, deg.
.8
.6
.4
.2
0
2
4
6
8
10
12
14
STATIC FORCE AND MOMENT COEFFICIENT DERIVATIVES AT $\beta = 0$
(FOR DETERMINING CENTER OF PRESSURE ACCORDING TO SIMPLIFIED FLOW THEORY)
SHIP MODELS
PLATES

FIGURE 30

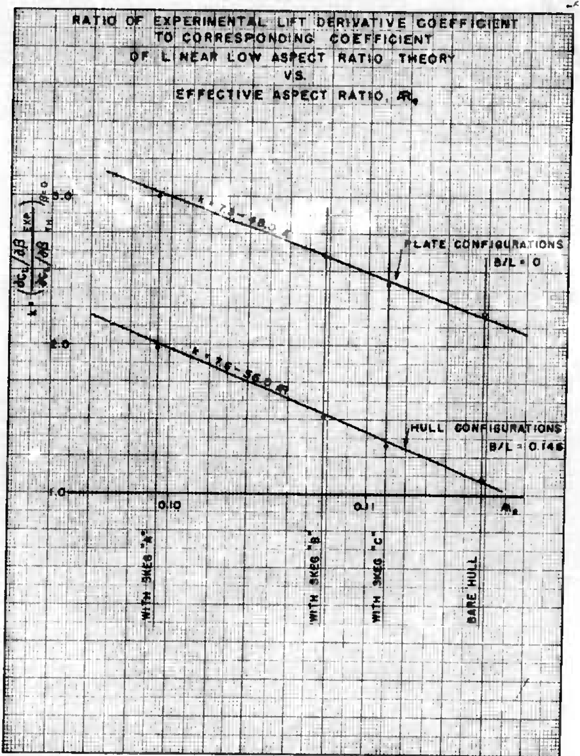
RATIO OF EXPERIMENTAL LIFT DERIVATIVE COEFFICIENT
TO CORRESPONDING COEFFICIENT
OF LINEAR LOW ASPECT RATIO THEORY
VS.
EFFECTIVE ASPECT RATIO
3.0
2.0
1.0
0.10
PLATE CONFIGURATIONS
B/L = 0
HULL CONFIGURATIONS
B/L = 0.146
WITH SKEG "A"
WITH SKEG "B"
WITH SKEG "C"
BARE HULL

FIGURE 31

APPENDIX A

Figures A-1, A-2, A-3

SCHEMATIC DRAWING OF MODEL WITH VARIOUS SKECS

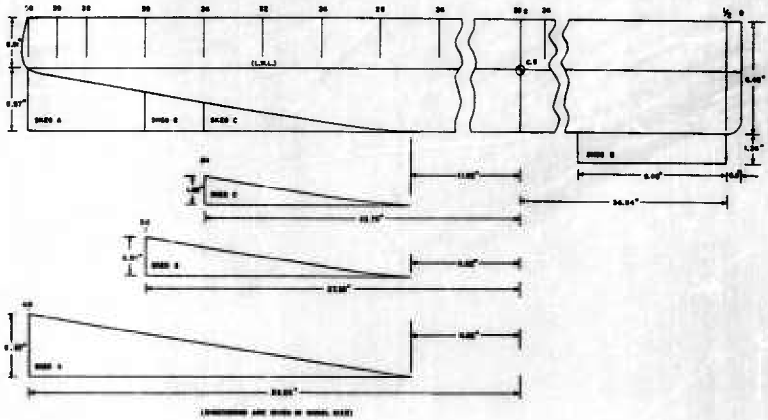

FIGURE A - I

FIGURE A-2
MODEL AND TOWING APPARATUS

FIGURE A-3
PLATE AND TOWING APPARATUS